1-1-2001

Applications of inductively coupled plasma mass spectrometry to the analysis of biomolecules

Yongjin Hou
Iowa State University

Applications of inductively coupled plasma mass spectrometry to the analysis of biomolecules

by

Yongjin Hou

A thesis submitted to the graduate faculty

in partial fulfillment of the requirements for the degree of

MASTER OF SCIENCE

Major: Analytical Chemistry

Major Professor: Dr. R.S. Houk

Iowa State University

Ames, Iowa

2001

Graduate College

Iowa State University

This is to certify that the Master's thesis of

Yongjin Hou

has met the thesis requirements of Iowa State University

Signatures have been redacted for privacy

TABLE OF CONTENTS

LIST OF FIGURES

LIST OF TABLES

1. GENERAL INTRODUCTION

An investigation of the dynamic interactions between DNA and two specific metals (uranium and holmium) is the first research topic of the thesis so the basic information regarding metal-DNA interactions is presented first.

DNA-metal interaction

Metal-DNA interaction is a research area that is attracting the interest of more and more scientists, due to many practical motivations, such as pharmaceutical applications [1-10], toxicity concerns [7, 11-13], DNA probe design [1, 14] and DNA purification [15, 16].

As we know, the four bases of DNA are adenine (A), guanine (G), cytosine (C), and thymine (T). Their structures and labeling are in Fig 1.

Coordination, intercalation and hydrogen bonding are the three fundamental DNA-metal interactions. Most coordination interactions between DNA and metals involve soft metal ions and nucleophilic positions on the DNA bases. The structure of cis- $(NH_3)_2$Pt-dGpG is a classical example: its platinum center coordinates to the N7 position of the guanine bases [5]. Other nucleophilic sites on DNA suitable for soft metals include the N7 position of adenine, the N3 position on cytosine, and the deprotonated N3 position on thymine [7]. Hard transition-metal ions are capable of coordinating to the phosphate oxygen atoms [17]. In some rare cases, the sugar ring, which is a poor ligand, is involved in the coordination [18-20]. Besides direct coordination, non-covalent metal-DNA interactions are also important, such as intercalation and hydrogen bonding [21-23]. In the intercalation mode, metal ions or complexes are slotted into the double planar layers of ligands, just like the meat in the middle of a sandwich. It is not surprised that the ligands of the metal

complexes can form hydrogen bonds with polynucleotides, especially with the phosphate oxygen. A mix of covalent and non-covalent bonding is possible.

There are two fundamental categories of reactions between transition metal complexes and DNA: (1) redox reaction; (2) hydrolytic reaction.

The Fenton reaction is the simplest and most classic example of the redox reactions. In the Fenton reaction, the metal doesn't directly attack polynucleotides but it helps to generate OH radicals, which will attack and cleave the DNA chains. A Fenton reaction involving Fe^{3+} ions is:

$$Fe(II) + H_2O_2 \text{ -----> } Fe(III) + OH^{\cdot} + OH^{-}$$

$$Fe(III) + e^{-} \text{ ----> } Fe(II)$$

Fenton reactions can be site-nonspecific and also can be designed to be site-specific. Dervan and coworkers made the first demonstration of site-specific Fenton reactions [24]. Like Fenton reactions, other redox reactions use the oxidative material produced in some early step of reactions to cleave DNA chains. Both the sugar and base can be the target of reactions.

Hydrolysis of nucleic acids mediated by metal ions is important in natural enzymatic reactions [7]. If a metal ion can function like a Lewis acid, then it is potentially effective in promoting hydrolysis of the phosphodiester by polarizing the phosphorus-oxygen bond.

The metal-DNA interactions have been applied to spectroscopic probes, metallofootprinting reagents, conformational probes, and anti-cancer drugs. The tris (phenanthroline) ruthenium (II) complexes offer a novel spectroscopic probe of nucleic acids, since the intensity and frequency of luminescence are increased upon intercalation into the

double helix. As a result the complexes provide a simple luminescent stain for DNA in fluorescent microscopy experiments [7].

Utilization of metal complexes for chemical footprinting is a very important application in biology. Initially biologists developed the footprinting technique as a means of locating protein-binding sites on DNA [25]. The basic idea of this technique is that once a position on the DNA helix is attached by metalloproteins, then bonded spot is unavailable for redox cleavage. The comparison of protein-bonded mapping of DNA and nonprotein-bonded mapping tells the protein-binding sites on DNA. A simple footprinting reagent of great utility is $Fe(EDTA)^{2-}$ [26]. Since this dianion is unlikely to bind with the DNA polyanion, the hydroxyl radicals produced via Fenton reaction at a distance from the DNA helix would likely diffuse and distribute along the helix evenly. So the result is a completely sequence-neutral pattern of cleavage. The very small hydroxyl radicals can even diffuse within the DNA-binding protein to delineate binding domain and consequently the footprinting resolution is extremely high. Other footprinting reagents in use include $Cu(phen)_2$ and manganese porphyrins [27-29].

X-ray crystallography is the critical method of finding conformation information about the DNA double helix. Yet many conformations have still not been described to high resolution, and only a few oligonucleotides have been crystallized. Other techniques are therefore required to bridge the small set of oligonucleotide crystal structures that point to plausible structures and the large array of structures that arise as a function of sequence on long helical polymers [7]. Metal complexes can be used as both nonspecific conformation probes and shape-selective probes. OsO_4 can react across the 5,6 position of accessible pyrimindines to form cis-osmate esters [7]. Hence DNA containing unusual local

conformations with prominent solvent-accessible pyriminides can be probed with OsO_4. The junction regions of Z-DNA, the single-stranded loops in cruciform structures, and a segment of the dangling third strand in H-DNA have all been probed by means of the differential reactivity of osmium tetroxide with DNA sites dependent upon their accessibility [7].

Metal complexes have been explored as anticancer drugs, and it has been known that DNA is the direct target of metal complexes for its anti-tumor effectiveness [1-6]. Interestingly, the anti-tumor function of metal complexes is due to the toxicity of those heavy metals. Amazingly, metal complexes of proper dose are more toxic to DNA in tumor cells than to those in normal cells, and that is why the metal complexes are effective in killing tumors. Platinum, gold, ruthenium, rhodium and other transition metal compounds have been developed for this use [1-6]. The main considerations in designing this kind of medicine are to make it absorbed easily by cells with less side effects (e.g. kidney toxicity and neurotoxicity).

Size exclusion chromatography

Size exclusion chromatography (SEC) is also called gel permeation chromatography (GPC). In SEC solutes are separated as a result of their permeation into solvent-filled pores by virtue of their physical size. Smaller molecules permeate more deeply the pores. As a general rule, bigger molecules elute out earlier than smaller molecules. By far SEC is one of the most popular and convenient methods of determining the average molecular weight and the molecular weight distribution of a polymer [30]. Although DNA fragments are usually separated by gel electrophoresis, size exclusion provides an alternative method, which is reproducible and straightforward to interface to ICP-MS.

Size exclusion was first noted in the late 1950s when separation of proteins on column packed with swollen maize starch was observed [31-33]. The run time was typically 48 hours. Recently SEC has been developed on three lines. The first line of development addressed the need for media of different separation ranges since the separation range solely depends on the pore size distribution of the media. The second line of development was to decrease the particle size, which is the key factor in decreasing separation time. The third line was to make the pore size distribution more uniform, which can dramatically increase the selectivity and resolution.

In SEC, the first consideration in selecting the mobile phase is the solubility and compatibility between the mobile phase and solutes, though secondary effects, such as ionic and hydrophobic effects, may exist. The SEC eluent can be organic free, and it can be prepared as a buffer around pH 7. These features of SEC along with the ease of correlating retention time to molecular weight make SEC effective for separating bio-molecules even though the resolution of SEC is usually not great. One way to improve the resolution of SEC is to combine several columns in line but the elution time increases as compensation.

Next, the technique and instrument used for detecting metals in my experiments are described.

Introduction to inductively coupled plasma mass spectrometry (ICP-MS)

ICP-MS is the art of combination, which was initially made by R. S. Houk at the Ames Laboratory.

The inductively coupled plasma is an electrodeless discharge at atmospheric pressure, supported by a radio frequency generator. Argon is the most commonly used gas, although others are occasionally used [34-37]. Basically there are three gas flows going through the

torch, and they are the outer gas flow (10 –15 L/min), intermediate flow (~ 1 L/min) and aerosol gas flow (~ 1 L/min). The extreme heat in the plasma (temp. higher than 5000 K) gets the introduced sample aerosol vaporized, atomized, excited and ionized. Then the ions that are mostly singly charged are extracted through the sampler and skimmer cones into the mass spectrometer.

Various mass spectrometers can be combined with the ICP. The quadruple analyzer is rugged and cheap but has relatively low mass resolution [38]. The electrostatic analyzer is commonly used as the energy selector while the magnetic sector mass analyzer is used as the mass selector [39-42]. The marriage of magnetic sector and electrostatic analyzer allows high resolution MS.

ICP-MS has many valuable features which include very low detection limits (ppt to ppq level for most elements), fast data acquisition, large linear dynamic range, simple, easily interpreted spectra, and the ability to couple with other sample introduction options, such as laser ablation, liquid chromatography. The features of ICP-MS itself and its further combination accounts for its popularity. ICP-MS has not only been used for trace and ultra-trace elemental analysis but also has been involved in biomedical research, food nutrition, geochemistry, environmental sciences, pharmaceutical quality control, semiconductor industry, clinical toxicology, forensic science, etc. [43-62].

Just ten years ago, some problems with ICP-MS, such as mass bias, matrix effects, polyatomic interference, and loss of ions during transportation from sampling still limited its use [63-65]. But now these problems have been solved or alleviated to some extent, due to modern automation, electronics and enriched knowledge in chemistry. ICP-MS is a very mature technique now.

Magnetic sector ICP-MS

The sector ICP-MS usually promises high mass resolution due to the double focusing by the magnetic sector and electrostaic analyzer. The Finnigan MAT Element is a commercialized sector ICP-MS instrument. Its mass analyzer is of reversed Nier-Johnson geometry, which means a 60° magnetic sector precedes a 90° electrostatic analyzer. As claimed by the manufacturer, the specifications of Element 2 are in shown in Table 1.

Table 1. Element 2 specifications

Sensitivity (concentric nebulizer)	1 x 10^9 cps/ppm In
Detection Power	< 1 ppq for non-interfered nuclides
Dark Noise	< 0.2 counts / seconds [cps]
Dynamic Range	> 10^9 linear with automatic gain calibration
Mass Resolution	300, 4000, 10000 (10 % valley), DS controlled
Signal Stability	better 1 % over 10 minutes
Signal Stability	better 2 % over 1 hour
Scan Speed (magnetic)	m/z 23->240->23 in less than 355 sec
Scan Speed (electric)	1 ms/jump, independent of mass range

The second project of my research is to develop the quantification method for phosphorous in proteins. Some historical facts and basic knowledge about phosphoprotein are introduced here.

Phosphoproteins

The first phosphoproteins to be discovered as early as in the 19th century were milk proteins of the casein family and the egg yolk protein phosvitin. For almost a century casein, phosvitin and some related milk and egg yolk proteins were the main phosphoproteins known. Consequently, protein phosphorylation was mainly regarded as a gross metabolic reaction. It was not until 1955, by Fischer and Krebs [66] and Sutherland and Wosilait [67], that the regulatory role of protein phosphorylation was shown.

Protein phosphorylation is a reversible process. It is catalyzed by protein kinase and reversed by protein phosphases. In the early 1980s, when great number of protein kinases were found, protein phosphorylation became recognized as the major general mechanism by which intracellular events in mammalian tissues are controlled by external physiological stimuli [68]. In bacteria, protein phosphorylation has been found to be targeted to Ser, Thr, Tyr, His, Arg, Lys, Asp, Glu, and Cys residues [69].

It is becoming apparent now that protein phosphorylation/dephsophorylation provides a major binary code for signal processing (i.e. decoding and interpretation) in cells. This mechanism, together with other chemical interactions, builds a tight communicative network between innumerable protein molecules. Such a network which in many aspects resembles a neuronal network, shows an amazingly high degree of redundancy, cross-talk and feed-back control of the signaling pathways which is a prerequisite for its plasticity, i.e. its ability to adapt and to learn [70].

Thesis organization

This thesis consists of four chapters: 1) the general introduction 2) a paper prepared for scientific journal 3) another paper prepared for scientific journal 4) the general

conclusion. Chapter 2 and 3 have their own abstracts, introductions, conclusions, acknowledgements and references.

References

1. Jin L. and Yang P., *Journal of Inorganic Biochemistry*, 1997, **68**, 79-83.
2. Gonzalez V. M., Perez J. M. and Alonso C., *Journal of Inorganic Biochemistry,* 1997, **68**, 283-287.
3. Alessio E. and Iengo E. et al., *Journal of Inorganic Biochemistry*, 2000, **79**, 173-177.
4. Gunus F. and Algul O., *Journal of Inorganic Biochemistry*, 1997, **68**, 71-74.
5. Suzanne E. Sherman, Dan Gibson, Andrew H.-J. Wang, Stephen J. Lippard, *Science*, 1985, **230**, 412-417.
6. Rosenberg B., VanCamp L., Trosko J., Mansour V., *Nature*, 1969, **222**, 385.
7. Bertini I., Gray H. B., Lippard S. J. and Valentine J.S., *Bioinorganic Chemistry*, **1994**, chapter 8, 455-503.
8. Roberts J. J. and Thomson A. J., *Progress in Nucleic Acid Research and Molecular Biology,* 1979, **22**, 71-133.
9. Pinto A. L. and Lippard S. J., *Biochimica et Biophysica Acta,* 1985, **780**, 167-180.
10. Sherman S. E. and Lippard S. J., *Chemical Reviews,* 1987, **87**, 1153-1181.
11. Kazimierz S. Kasprzak and Miral Dizdaroglu et al., *Carcinogenesis*, 1997, **18**, 271-277.
12. Conte, C., Mutti, I., and Marmiroli, N., et. al., *Chemosphere*, 1998, **37**, 14.
13. Monika Asmuss, Leon H.F. Mullenders, Andre Eker and Andrea Hartwig, *Carcinogenesis*, 2000, **21**, 2097-2104.
14. Peter Leverett, Janice Petherick and Robert S. Vagg., et. al., *Journal of coordination chemistry*, 1999, **49(2)**, 91-100.

15. Nandi U. S., Wang J.C. and Davidson N., *Biochemistry*, 1965, **4**, 1687.

16. Harald Biersack, Sanne Jensen and Ole Westergaard, *Methods in Molecular Biology*, 1999, **94**, 235-242.

17. G. L. Eichhorn and Y. A. Shin, *J. Am. Chem. Soc.* 1968, **90**, 7323.

18. L. G. Marzilli, *Prog. Inorg. Chem.* 1977, **23**, 255.

19. C. H. Chang, M. Beer, and L. G. Marzilli, *Biochemistry* 1977, **16**, 33.

20. Glikin et al. *Nucleic Acids Res.* 1984, **12**, 1725.

21. M. B. Fleisher, H. Y. Mei, and J. K. Barton, *Nucleic Acids and Mol. Biol.* 1988, **2**, 65.

22. S. J. Lippard, *Acc. Chem.* Res. 1978, **11**, 211.

23. R. V. Gessner et al., *Biochemistry* 1985, **24**, 237.

24. P. B. Dervan, Science 1986, **232**, 464.

25. M. D. Purugganan et al., *Science*, 1988, **241**, 1645.

26. T. D. Tullius et al. *Methods in Enzym.* 1987, **155**, 537.

27. J. C. Dabrowiak, B. Ward, and J. Goodisman, *Biochemistry*, 1989, **28**, 3114.

28. R. Law et al. *Proc. Natl. Acad. Sci.* USA, 1987, **84**, 9160.

29. C. L. Peterson and K. L. Calane, *Mol. Cell Biol.* 1987, **7**, 4194.

30. Sadao Mori and Howard G. Barth *Size Exclusion Chromatography*, Springer, **1999**, p4

31. Chi-San Wu, *Column Handbook for Size Exclusion Chromatography*, Academic Press, **1999**, p27.

32. Lindqvist, B. and Storgards, T. *Nature*, 1955, **175**, 511.

33. Lathe, G. H. and Ruthven, C. R., *Biochem. J.*, 1956, **62**, 665-674.

34. Evans, E. H., Giglio, J. J., Castillano, T. M. and Caruso, J. A. *Inductively Coupled and Microwave Induced Plasma Sources for Mass Spectrosocopy*, Royal Society of

Chemistry, UK, **1995**.

35. Blades, M. W., Weir, D. G. *Spectrosc* 1994, **9(8)**, 14.
36. Hieftje, G. M., Galley, P. J.; Glick, M.; Hanselman, D. S. *J. Anal. At. Spectrom.* 1992, **7**, 69.
37. Hieftje, G. M. Spectrochim. Acta 1992, **47B**, 3.
38. Peter H. Dawson, Quadruple mass spectrometry and its applications, **1976**
39. Mones and Jakubowski, *Anal. Chem.,* 1998, **70**, 251A-256A.
40. Douthitt, *ICP Inform. Newsletter* 1999, **25(2)**, 87-120.
41. Becker and Dietze, *Spectrochim. Acta B* 1998, **53**, 1475-1506.
42. C. A. McDowell, *MS*, **1963**, p210.
43. Houk, R. S., Shum, S. C. K.; Wiederin, D. R. *Anal. Chim. Acta.* 1991, **250**, 61.
44. Olesik, J. W. *Anal. Chem.* 1991, **63**, 12A.
45. Turner, P. J., *Application of Plasma Source Mass Spectrometry*, Royal Society of Chemistry, UK, **1991**, p71.
46. Tanner, S. O., Cousins, L. M., Douglas, D. *J. Appl. Spectrosc.* 1994, **48**, 1367.
47. Kornblum G. K. and De Galan, L. *Spectrochim. Acta* 1977, **32B**, 71.
48. Montaser. A. and Golightly, D. W. Inductively Coupled Plasma in Analytical Atomic Spectrometry, VCR Publishers, **1992**.
49. Kalnicky, D. J., Excitation Temperature and Electron Number Density Distrubutions Experienced by Analyte Species in an Inductively Coupled Argon Plasma, Chemistry Department, Iowa State University, **1976**.
50. Jarvis, K. E., Gray, A. L. and Houk, R. S., *Hankbook of Inductively Coupled Plasma Mass Spectrometry*, Blackie, New York, **1992**.

51. Boumans, P. W. *Spectrochimi. Acta* 1982, **37B**, 75.

52. Douglas, D. J. and French, J. B. *J. Anal. At. Spectrom.* 1988, **3**, 743.

53. Niu, H. S., Hu, K. and R. S. Houk *Spectrchim. Acta* 1991, **46B**, 805.

54. Shen, K. L. and Fu, C. C., *Spectrochimi. Acta*. 1990,**45B**, 527.

55. Douglas, D. J. and French, J. B. *Anal. Chem.*, 1981, **53**, 37.

56. Houk, R. S.; Fassel, V. A., Flesch, *Anal. Chem.*, 1980, **52**, 2283.

57. Olson, L. K. and Caruso, J. A. *Spectrochim. Acta*. 1994, **49B**, 7.

58. Olivares, J. A. and Houk, R. S., *Anal. Chem.*, 1986, **58**, 20.

59. Chen. X. and Houk, R. S., *Spectrochim. Acta*, 1996, **51B**, 41.

60. Date. A. R., Cheung, Y. Y. and Stuart, M. E., *Spectrochim. Acta*, 1987, **42B**, 3.

61. Wilson, D. A., Vickers, G. M., Hieftje, G. M. and Zander, A. T., *Spectrochim. Acta*, 1987, **42B**, 29.

62. Denoyer, E. R., Jalys, M. D., Debrach, E. and Tanner, S. D., *At Spectrosc.*, 1995, **16**, 1.

63. Beauchemin, D., Mclaren, J. W. and Berman, S. S., *Spectrochim. Acta*, 1987, **42B**, 467.

64. Evans, E. H. and Giglio, J. J., J. *Anal. At. Spectrom.*, 1993, **8**, 1.

65. Smith, F. G., Weiderin, D. R. and Houk, R. S. *Anal. Chem.* 1991, **63**, 1458.

66. E. H. Fischer, E. G. Krebs, *J. Biol. Chem.* 1955, **216**, 121-132.

67. E. W. Sutherland, W. Y. Wosilait, *Nature*, 1955, **175**, 169-170.

68. P. Cohen, *Nature*, 1982, **296**, 613-620.

69. A.J.Cozzone, *J. Cell. Biochem.* 1993, **51**, 7-13.

70. Friedrich Marks, *Protein Phosphorylation*, VCH, **1996**.

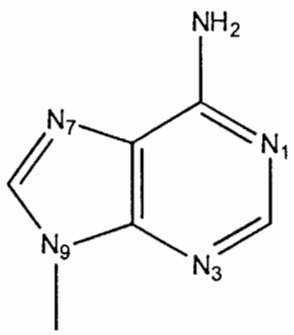

adenine

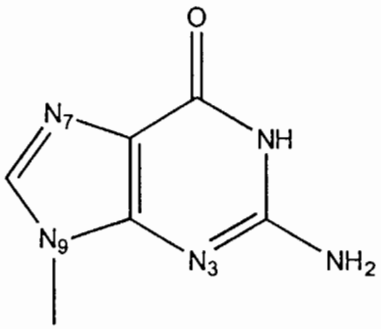

guanine

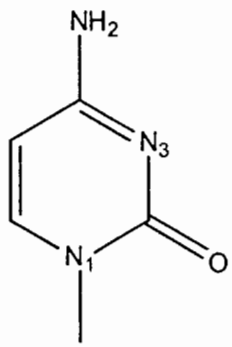

cytosine

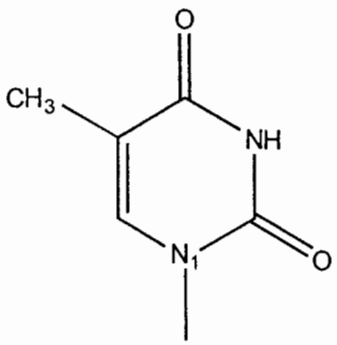

thymine

Fig 1 bases and their labelings

2. MEASUREMENT OF KINETICS OF BINDING BETWEEN URANIUM OR HOLMIUM AND DNA BY SIZE EXCLUSION CHROMATOGRAPHY INDUCTIVELY COUPLED PLASMA MASS SPECTROMETRY

A paper to be submitted to Bioinorganic Chemistry

Yongjin Hou and R. S. Houk

ABSTRACT

To make a dynamic investigation on the interactions between DNA and uranium/holmium, we spiked metals at low ppb level into solutions of 5ppm DNA. The experiments were performed near physiological conditions, so the activeness and attributes of DNA were maintained, and the best imitation of what could happen between DNA and uranium/holmium in natural surroundings was obtained. Inductively coupled plasma mass spectrometry (ICP-MS) made it possible to determine the metals at ultra-trace level. Size exclusion chromatography (SEC) column was employed to separate DNA fragments. We not only determined the sizes of DNA fragments that could bond to uranium/holmium under our experiment conditions but also measured the amount of metals bound to DNA fragment verse time. By this way, a dynamic view of DNA-uranium/holmium interactions was obtained, which provided information concerning the rate and equilibrium of interactions. Essentially, an accurate and reliable calibration to determine the size of unknown DNA fragments was required. A calibration done with DNA markers was compared with one done with protein markers. It turned out it was more accurate and reliable to use DNA markers to calibrate unknown DNA fragments.

INTRODUCTION

Metal-DNA interaction is a burgeoning field of research due to many practical motivations. Among them, there are pharmaceutical applications [1-10], toxicity concerns [7, 11, 12, 13], DNA probe design[7, 14] and DNA purification[15, 16]. Going over the previous research on metal-DNA interactions, we noticed that main group metals (including Na, K Mg, Ca, Sn etc.) and transition group metals (including Fe, Co, Ni, Zn, Cd, Hg, Cu, Ag, Au, Os, Ru, Rh, V, Mn, Pt, Pb etc.) have received much more attention than the actinide elements. Previous research mostly reported the existence or specification of interaction. Records on kinetic attributes of interactions (e.g. the rate of interaction and equilibrium of interaction) are rarely seen.

The occurrence of actinide elements is ubiquitous and they are well known as environmental hazards. Uranium is the most abundant actinide element in nature and it is the one used most commonly in industry. As reported, uranium occurs naturally at an average of 3μg/L in seawater, and continental surface waters contain 0.1 to 500 μg/L U [18]. Mining, nuclear waste disposal and tank-armor of depleted uranium [19] expose certain groups of people to surroundings of even higher level of this element. Uranium is a general cellular poison and can potentially affect organs and tissues when it is accumulated to certain amount in biological media. The hazards associated with uranium exposure include both chemical toxicity and radioactivity. Due to long half lives of uranium isotopes (^{238}U: 4.49 x 10^9 yrs, ^{235}U: 7.10 x 10^8 yrs, ^{234}U: 2.48 x 10^5 yrs), radiobiological damage from U is of chronic effect, compared with its chemical hazard [19]. A soft α-particle emitter, uranium is more dangerous as an internal radiological hazard than as an external hazard. Uranium can enter the human body by the oral route (in food and water), by inhalation, and through the skin and

mucous membranes [17]. Finally, it deposits in human organs, for example, lung, liver and bone [17].

Like the information above, most previous documents concerning hazards associated with uranium include cells, tissues or organs, i.e. mostly systems much larger than individual molecules. To understand the underlying reasons of the chemical toxicity of uranium, it is important to know how uranium affects DNA, the genetic pathway. A few papers concern the uranium-DNA interactions [20-23]. Those research, however, focused on how to use uranyl (VI) as a DNA- probe and they were mainly done with acidic condition, ultraviolet irradiation, and most soluble species of uranium compounds. In our opinion, the uranium-DNA interaction under this kind of experimental conditions may not represent the real case in nature.

The actinide elements after uranium hardly occur in nature but it doesn't mean they don't exist around us or their effects on biological systems can be ignored. Plutonium is used in nuclear weapons and power reactors and its side products, such as americium and curium cause many of the long-term radiological and thermal problems associated with reactor waste storage and disposal [24]. Believe it or not, in the USA, an expanding use of americium is in smoke-detector alarms [24]. These post-uranium elements are radioactive hazards while documents regarding their chemical effects on biological systems are barely seen. Neptunium and plutonium, the two elements right after uranium, are similar to uranium chemically [25]. Afterwards, starting from americium, the following actinide elements have characteristic valence of +3 in aqueous solutions as lanthanide elements do, and they chemically resemble lanthanide elements [25]. So it is possible that the chemical effects of lanthanide elements on biological systems resemble those of americium, curium, berkelium and so on.

In our present work, uranium was chosen due to its importance in industry and widespread occurrence. Holmium, which has only one isotope (^{165}Ho) was picked due to the chemical similarity between lanthanide elements and post-uranium actinides elements and due to the low natural abundance of holmium. SEC and ICP-MS were put in line. The trace amount of metals used in our work was designed to be representative of the low concentrations of these metals in environment. The interaction between DNA and uranium or holmium happened in tris-HCl buffer at pH 7.3, which is close to the real physiological condition. Molecule separations in SEC columns were done with the same buffer. The magnetic sector ICP-MS promised us extremely low detection limit and online chromatography. By integrating the chromatography peak areas of U, Ho detected by ICP-MS, we could determine the amount of metals bound to DNA fragments. With a series of measurements done over time, the dynamic plots for DNA's interactions with U and Ho were respectively obtained. By making a SEC calibration curve, the retention time and molecular weight of eluted peaks could be determined.

In short, our work attempted to mimic the real situation that may occur between DNA molecules and U/Ho. We hope that our work can enlarge the knowledge about metal-DNA interactions to actinide metals and can be an early exploration to kinetics aspect of metal-DNA interactions. Our work may also be helpful to understand how U and Ho affect the health of biological systems at the molecular level.

EXPERIMENTAL

Instrumentation

Fig 1 describes the overall instrument setup. The instrumentation details including component models and operating conditions are listed in Table 1. Several things need to be

Table 1. Component models and operating conditions

Component	Operating Conditions
HPLC pump	0.5 ml/min
(Acuflow Series III pump)	
UV-VIS absorbance detector	260 nm or 280 nm
(Rainin Dymax)	
SEC column	mobile phase
(Tosohaas G 3000 SWXL, Dims. 7.8 mm x	0.05 M tris-HCl, pH 7.3, 0.05 % NaN_3
30 cm, particle size 5μ, pore size 250 A)	
Guard column	
(Tosohaas Dims. 6 mm x 4 cm)	
Injection valves (pre and post columns)	
(Rheodyne Metal Free 9725 i with 20 μl loop)	
Nebulizer	natural uptake rate: 100 μl/min
(PFA 100)	but pumped at flow rate of 0.5 ml/min
ICP-MS	low resolution: nominally, 300
(Finnigan Element)	RF power: 1200 kW
	outer argon flow: 15 L/min
	auxiliary: typically 0.65 L/min
	aerosol flow rate: typically 0.95 L/min
Condensor	2 °C

pointed out. First, we skipped the heater, which usually precedes the condenser since the heater could worse the signal stability while improving the sensitivity. Second, low resolution (nominally, $m/\Delta m=300$) was usually used because there are no polyatomic interferences for $^{238}U^{+}$ and $^{165}Ho^{+}$. Just in one experiment of detecting $^{31}P^{+}$and $^{238}U^{+}$ simultaneously, medium resolution was chosen. Third, to gain the best balance between signal sensitivity and signal stability, the aerosol flow rate and the auxiliary flow rate were tuned each time when the instrument was used. The values in Table 1 are just the typical ones.

Reagents and solutions

The stock solutions of uranium and holmium were from SPEX. The HPLC buffer was 0.05 M tris-HCl plus 0.05% NaN_3, pH 7.3. The buffer was also used to dilute DNA, uranium and holmium solutions. DNA Molecule Marker V from Boehringer Mannheim, consisted of 22 fragments ranging from 8 bp to 587 bp. Instead of being used as the marker, it was diluted in buffer and then either uranium or holmium solution was spiked into the diluted DNA. Finally, the mixture dissolved in buffer was 5 ppm Marker V plus 1 ppb uranium or 5 ppm Marker V plus 0.5 ppb holmium. The protein markers from Sigma included carbonic anhydrase, bovine erythrocytes (29 K), albumin, bovine serum (66K), alcohol dehydrogenase, yeast (150 K), β-Amylase, sweet Potato (200 K) and thyroglobulin, bovine (669 K). The short, single-stranded DNA chains made by the DNA facility of ISU were annealed into DNA fragments of 5 bp, 20 bp and 50 bp separately. Using enzyme restriction cleavage of plasmid DNA, we obtained DNA fragments of 194 bp, 412 bp and 695 bp. The above six, separated DNA fragments of known size were then used as our DNA markers.

Measurements

Since the loop volume of both injection valves was 20 μl and we always used full-injection mode, which means injection volume is as least three times of the loop volume, theoretically 20 μl did go through the injector without dilution each time. Either UV absorbance or ICP-MS was chosen exclusively as the detection method.

UV Detector

The protein weight markers (29 K, 66K, 150 K, 200 K, 669 K) were individually dissolved in buffer at roughly 1000 ppm. Then they were injected into the pre-column injection valve one by one. Meanwhile, UV absorbance was collected by a computer running with a homemade LABVIEW program at acquiring rate of 1 point/second. The UV wavelength was set to 280 nm. To ensure the chromatography of each injection was not interfered by that of the previous injection, a new injection was always performed 30 minutes after the previous one. The above part was the protein calibration, from which Fig 2 and curve A of Fig 3 were generated.

Similarly, we injected the DNA markers (5 bp, 20 bp, 50 bp, 194 bp, 412 bp, 695 bp) into the SEC column and obtained the DNA calibration (Fig 4 and curve B of Fig 3). The detector wavelength was 260 nm. The approximate concentration of 5 bp, 20 bp and 50 bp was 1000 ppm each. It was roughly 100 ppm each for 194 bp, 412 bp and 695 bp.

ICP-MS

With our method file for $^{238}U^{+}$, it took about 1.4 seconds to get one chromatography point while for $^{165}Ho^{+}$, it took about 1.2 seconds. As mentioned earlier, the uranium mixture was 5 ppm DNA spiked with 1 ppb uranium. Thirty minutes after the above mixture was prepared, the mixture was first injected and the data acquisition was started for $^{238}U^{+}$ with our

ICP-MS. About 20 minutes later, the signal of $^{238}U^{+}$ started rising. It turned out there was one small but significant peaked centered at 1320 seconds. The data acquisition was not stopped until the whole chromatography was complete, which took 30 minutes. Shortly, a uranium standard of 1.0 ppb was injected into post-column injection valve three times, each injection being separated by 20 seconds. So by comparing the area of chromatography peak from the mixture with that from uranium standard, we could quantify how much uranium was contained in the eluted fractions from the mixture. More injections were made after 1.5 hours, 2.5 hours, 4.5 hours, 6.5 hours, 8.5 hours, 26.5 hours and 47 hours. The uranium standard was injected post column after each injection. Besides the spiked DNA, 5 ppm pure DNA marker V was injected.

The mixture of 5 ppm DNA plus 0.5 ppb Ho was basically treated the same way. The difference was the time interval. For holmium, injections were made after 10 minutes, 30 minutes, 1 hour, 2 hours and 4 hours. It must be pointed out that the 10-minute injection was made after all the other injections and was with a different batch of mixture of the same composition.

RESULTS AND DISCUSSION

Comparison of protein calibration and DNA calibration

Fig 2 is the chromatogram for protein weight markers and Fig 3 is the one for DNA markers. In both plots, some curves were shifted up for clarification but all curves actually had baseline around zero absorbance. It should be noticed that the size of proteins usually is expressed in the term of molecular weight (MW) while the size of DNAs is expressed in the term of base pair (bp). To make them comparable, in Fig 3 that combined the calibration

curves of both DNAs and proteins, we converted the bp of DNAs into MW, based on the knowledge that one bp of Na^+B-DNA weighs an average of 660 Da [26]. Fig 3 showes that DNA fragments elute much faster than proteins of same MW. It is consitant with expectation that DNA is more open and occupies more larger volume than protein of same MW. The sharp contrast in Fig 3 meant we couldn't trust protein weight markers for calculating the size of unknown DNA fragments even though protein markers of single size are commercially easier to get.

Uranium bound to DNA

Curve A of Fig 5A shows the chromatogram from the first injection from the uranium-DNA mixture. Curve B is the chromatogram of the same mixture after 4.5 hours based on the preparation time. They were similar at peak positions. Both peaks ranged from 1220 seconds to 1500 seconds, centered around 1320 seconds. They were different at the peak sizes. The 30-minute injection gave a smaller peak of $^{238}U^+$ compared with the 4.5-hour injection. All the other uranium injections (1.5 hours, 2.5 hours, 4.5 hours, 6.5 hours, 8.5 hours, 26.5 hours, 47 hours) also generated chromatography peaks at the same position. According to our DNA calibration, those are DNA fragments of 14 bp, 11 bp and 6 bp. One pure DNA mixture without being spiked with uranium was injected into column and gave us the Curve C, from which uranium was hardly seen.

By using the post-column injections, we quantified the uranium bound to DNA. The results were plotted in Fig 5B. The data at 0 hour was taken from the measurement of 5 ppm pure DNA. The amount of bound uranium reached its maximum, which was about 77 ppt at 4.5 hours. After that, the curve went down and reached its steady state at about 44 ppt. The peak on the plot was reproducible in three independent trials though the reason was

unknown. Keep it in mind that 1 ppb uranium had been spiked into 5 ppm DNA. So at the maximum, the bonding ratio was 77 ppt/1.0 ppb = 7.7% and at the equilibrium the bonding ratio was 44 ppt/1.0 ppb = 4.4 %. These results indicates that most of the uranium doesn't bind to DNA.

Holmium bound to DNA

Curve B, Fig 6A depicts $^{165}Ho^{+}$ in the spiked DNA. Curve A is the chromatogram from 5 ppm DNA, which contained Holmium at about 6 ppt. The chromatography peak ranged from 1250 seconds to 1600 seconds, centered around 1380 seconds. According to our calibration, 1250 seconds corresponded to a DNA fragment of 13 bp, 1380 seconds to 9 bp and 1600 seconds to 4 bp. The amount of holmium that could be detected in our DI water and buffer was less than 1 ppt. So the non-spiked DNA must get its holmium somewhere during transportation or storage. All other holmium-related injections had a single chromatography peak centered at 1380 seconds. Fig 6B, plots the amount of holmium bound to DNA verse time for all these injections. Apparently, the slope of the curve started sharp. The 10-minute injection almost made the maximum. After that, the curve levels off and the equilibrium amount of Holmium bound to DNA is about 0.22 ppb. The spiked sample contained 5 ppm DNA plus 0.5 ppb holmium so the bonding ratio at equilibrium was 0.23 ppb / 0.5 ppb = 46%.

Ion exchange in the column

We injected 0.5 ppb solution of free uranium and holmium buffered at pH 7.3 but couldn't see uranium or holmium elute through the column in several hours. On one hand, this could be regarded as another evidence that the chromatography peaks were from uranium or holmium bound to DNA rather than from free metals. However, it also meant that

the packing material of the SEC column could trap free uranium and holmium. Then 5 ppm pure DNA was injected into the column. No DNA fragments of any size were observed to pick up the free uranium or holmium trapped in the column. So it meant the binding between the column material and the metals was strong and it also meant that trapped uranium or holmium didn't appear in subsequent chromatograms.

Some further investigations of the behavioral of free uraniumn and holmium were made. Uranium and holmium at 0.5 ppb in different buffers were injected into the column. As shown in Fig 7A, with the amount of EDTA increasing and pH value decreasing, higher and higher percentage of free uranium and holmium was observed to flow out the column. The height of bars in first three cases was exaggerated a little bit so as to be shown and the real recovery ratios were zero for all of them. Fig 7B showed the chromatography of free uranium and holmium. It seemed free uranium was more reluctant than holmium to leave the column and holmium was in larger complex than uranium.

Effect of metal on retention time

Does the metal bound to DNA fragments change the retention time of DNA? In this experiment, 1.0 ppb uranium was spiked into about 50 ppm DNA fragment, all of which were 5 bp. After 24 hours, ICP-MS was employed to measure $^{238}U^{+}$ (medium resolution: 4000) and $^{31}P^{+}$ (medium resolution: 4000) in the metal-DNA complex. As shown in Fig 8A, the $^{238}U^{+}$ chromatography peak was at 1538 seconds, which was close to 1544 seconds, the position of the $^{31}P^{+}$ peak and they both were near the time measured by UV absorbance for the pure DNA fragment of 5 bp. It also needs to be mentioned that 100% percent uranium was bound to DNA fragment of 5 bp, according to our determination. This is because the

small DNA fragments were in large excess. Thus, metal bound to DNA didn't change retention time of DNA fragments significantly.

Small fragments and low bonding ratio

We found that, only small fragments in our DNA mixture bound to uranium (5-14 bp) and holmium (4-13 bp). Uranium at 0.5 ppb was also spiked to DNA fragments of single size, 20 bp but no uranium was observed to elute from column along with DNA fragments of this size, as shown in Fig 8B. The holmium spiked to DNA fragment of 20 bp generated the similar results. It meant uranium or holmium couldn't bond to big DNA fragments or the bonding was so weak that the metal bound to big fragments could be taken off in the column.

Since big fragments didn't effectively involved into the binding with uranium and holmium, the ability of small fragments' binding with metals and the amount of small fragments determined bonding ratios which turned out low, especially for uranium.

As reported, the predominating species of uranium compounds at pH 7.3 and normal pressure is UO_2, which can not be well dissolved in water [18]. As previous research shows, the solubility and transportability are determining factors that how much uranium can be absorbed by cells [17]. It may be also the case at the molecule level so the insolubility of uranium compound in our experimental conditions may be responsible for the low bonding ratio and speed between uranium and DNA.

Actually, the very low bonding ratio of uranium should be treated as good news. Natural DNA molecules are all much bigger pieces. The weak interaction between uranium and large molecules reduces the health risk from uranium exposure. DNA is the genetic material so its safety may have even more far-reaching meaning to the safety of the cell, and even the safety of the whole biological system.

CONCLUSION

From experiments and data analysis above, the following conclusions were reached:

1. Small DNA fragments (< 20 bp) prefer to bind with uranium and holmium in buffer pH 7.3. There is no bonding or there is very weak bonding between big DNA fragments and uranium/holmium.

2. Holmium bonding is much more quick and effective than uranium bonding. In buffer, less than 8% uranium was observed to bond to DNA while about 46% holmium was observed. Holmium bonding curve in our experiment conditions reached its maximum just in 10 minutes while uranium curve took hours.

3. To determine the size of DNA more accurately with SEC column, using DNA markers is better than using protein markers.

4. The SEC column allows the surrounding near the physiological condition so that DNA fragments can maintain their natural properties and activeness. ICP-MS promises the metal detection at ultra-trace level. SEC-ICP-MS makes the dynamic investigation on metal-DNA interactions possible. This combination can be used to determine the size of DNA fragments that have been bonded, and to quantify the amount of metals that have bonded to DNA fragments. This combination may also be useful for dynamic investigation of other bio-molecules, e.g. proteins.

5. Metal ions, M^{n+} may stick to SEC column. In this case, the elution peaks of free metals can not be observed at amicable conditions.

ACKNOWLEDGEMENTS

Ames Laboratory is operated for U.S. Department of Energy by Iowa State University under Contract No. W-7405-ENG-82.

RERERENCES

1. Jin L. and Yang P., *Journal of Inorganic Biochemistry*, 1997, **68**, 79-83.
2. Gonzalez V. M., Perez J. M. and Alonso C., *Journal of Inorganic Biochemistry,* 1997, **68**, 283-287.
3. Alessio E. and Iengo E. et al., *Journal of Inorganic Biochemistry*, 2000, **79**, 173-177.
4. Gunus F. and Algul O., *Journal of Inorganic Biochemistry*, 1997, **68**, 71-74.
5. Suzanne E. Sherman, Dan Gibson, Andrew H.-J. Wang, Stephen J. Lippard, *Science,* 1985, **230**, 412-417.
6. Rosenberg B., VanCamp L., Trosko J., Mansour V., *Nature,* 1969, **222,** 385.
7. Bertini I., Gray H. B., Lippard S. J. and Valentine J.S., *Bioinorganic Chemistry,* 1994, **chapter 8**, 455-503.
8. Roberts J. J. and Thomson A. J., *Progress in Nucleic Acid Research and Molecular Biology,* 1979, **22**, 71-133.
9. Pinto A. L. and Lippard S. J., *Biochimica et Biophysica Acta,* 1985, **780**, 167-180.
10. Sherman S. E. and Lippard S. J., *Chemical Reviews,* 1987, **87**, 1153-1181.
11. Kazimierz S. Kasprzak and Miral Dizdaroglu et al., *Carcinogenesis*, 1997, **18**, 271-277.
12. Conte, C., Mutti, I., and Marmiroli, N., et. al., *Chemosphere*, 1998, **37**, 14.
13. Monika Asmuss, Leon H.F. Mullenders, Andre Eker and Andrea Hartwig, *Carcinogenesis*, 2000, **21**, 2097-2104.
14. Peter Leverett, Janice Petherick and Robert S. Vagg., et. al., *Journal of coordination chemistry*, 1999, **49(2)**, 91-100.
15. Nandi U. S., Wang J.C. and Davidson N., *Biochemistry*, 1965, **4**, 1687.

16. Harald Biersack, Sanne Jensen and Ole Westergaard, *Methods in Molecular Biology*, 1999, **94**, 235-242.

17. Filov V.A., Bandman A. L. and Lvin B. A., *Harmful Chemical Substances*, 1993, **1,** Uranium and Its Compounds, p351-373.

18. Burns P.C. and Finch R., *Reviews in Mineralogy*, 1999, **38**, 220-253.

19. G. Bukowski, D. A. Lopez, and F. M. McGehee III: Uranium Battlefields Home & Abroad: Depleted Uranium Use by the US Department of Defense; Rural Alliance for Military Accountability, Progressive Alliance for Community Empowerment, Citizen Alert, (March 1993).

20. Peter E. Nielsen, Claus Jeppesen and Ole Buchardt, *Federation of European Biochemical Societies*, 1988, **235**, 122-124.

21. Claus Jeppesen and Peter E. Nielsen, *Nucleic Acids Research*, 1989, **17**, 4947-4956.

22. Peter E. Nielsen, Catharina Hiort and Bengt Norden, et. al., *Journal of the American Chemical Society*, 1992, **114**, 4967-4975.

23. Qinyuan Wu, Xueheng Cheng, Steven A. Hosfstadler and Richard D. Smith, *Journal of mass spectrometry*, 1996, **31**, 669-675.

24. Joseph J. Katz, Glenn T. Seaborg and Lester R. Morss, *The Chemistry of Actinide Elements, Second Edition, Volume 2,* 1986, p887.

25. F. Albert Cotton and Geoffrey Wilkinson, *Advanced Inorganic Chemistry, Third Edition,* 1972, p1084.

26. Donald Voet and Judith G. Voet, *Biochemistry, Second edition*, 1995, p860.

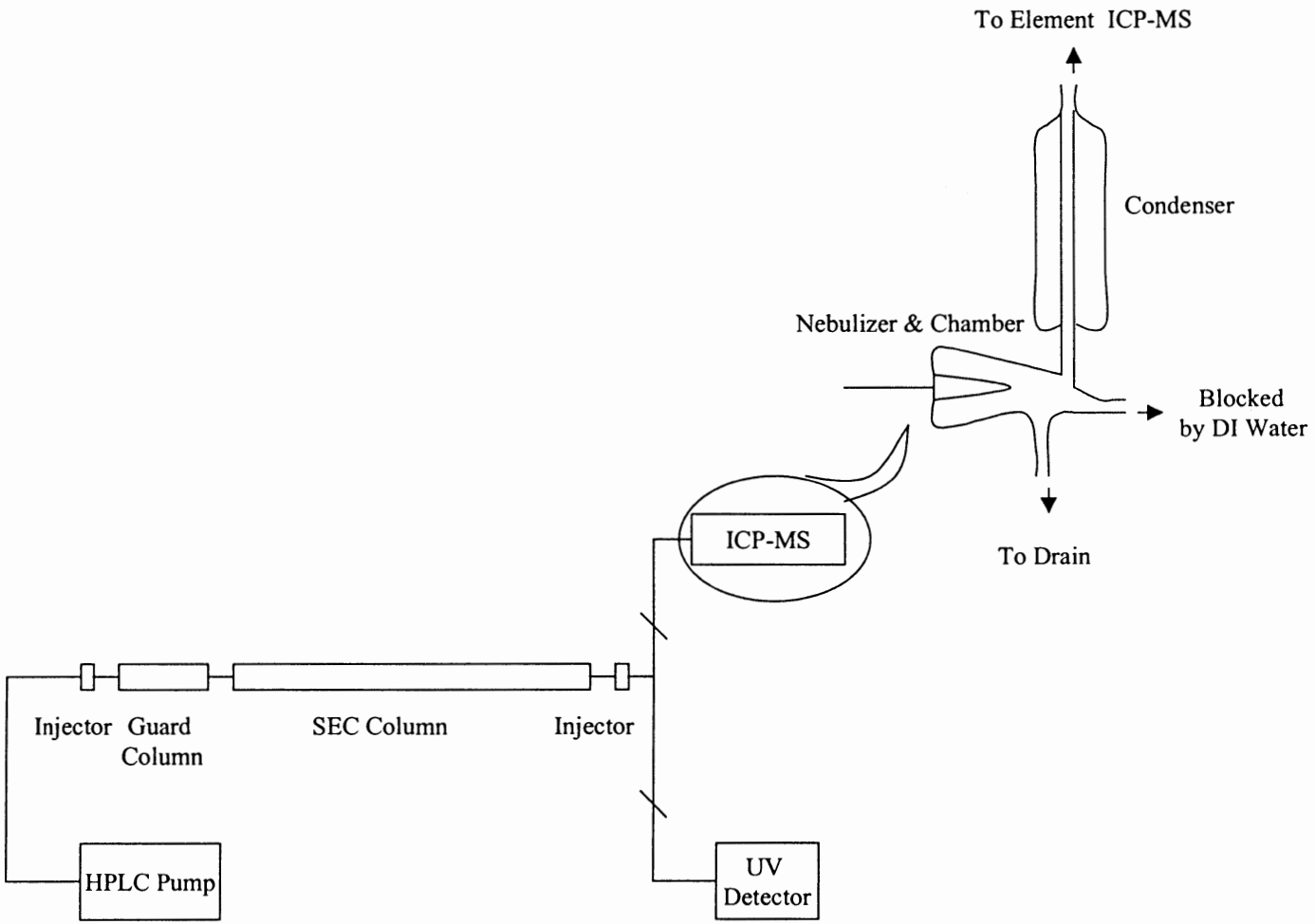

Fig 1 Overall instrument setup

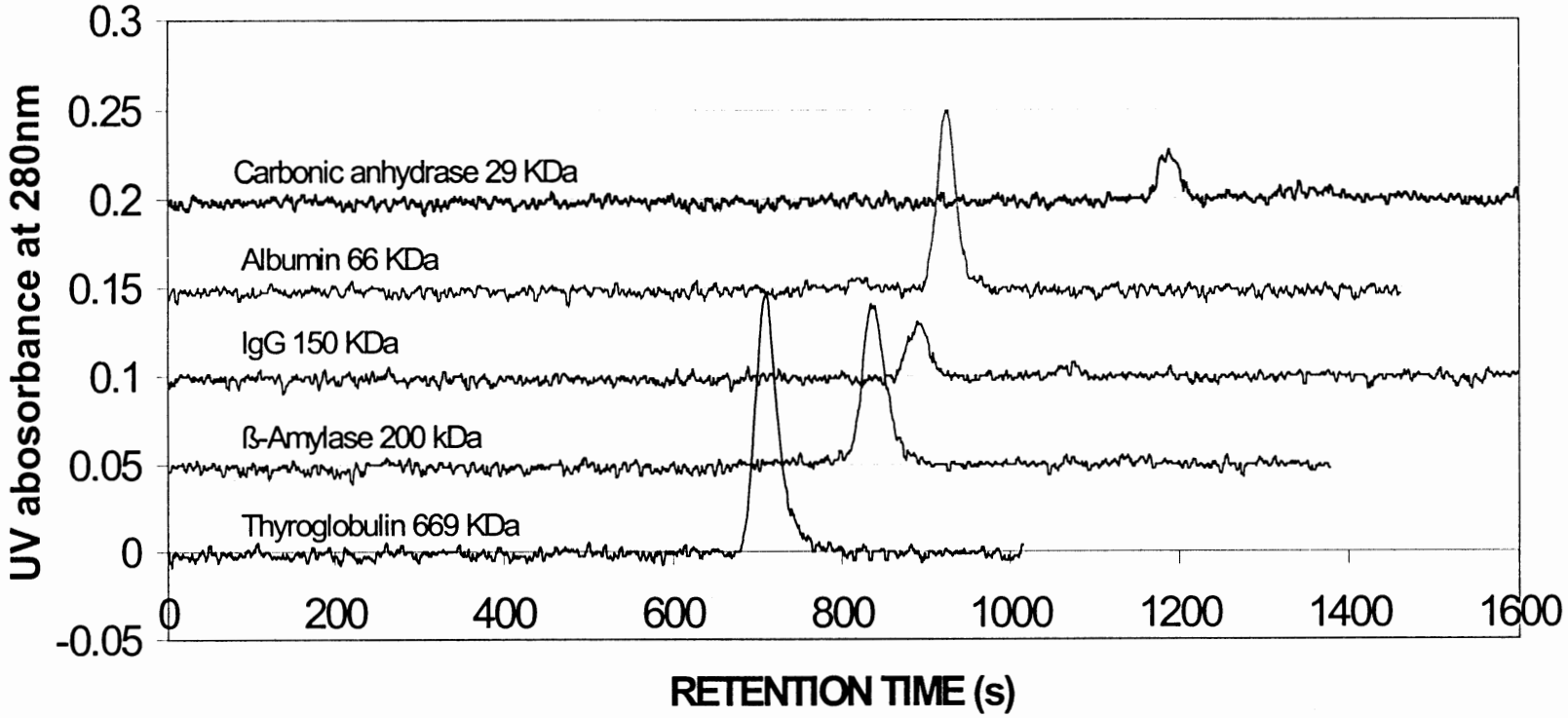

Fig 2 Chromatography of protein weight markers

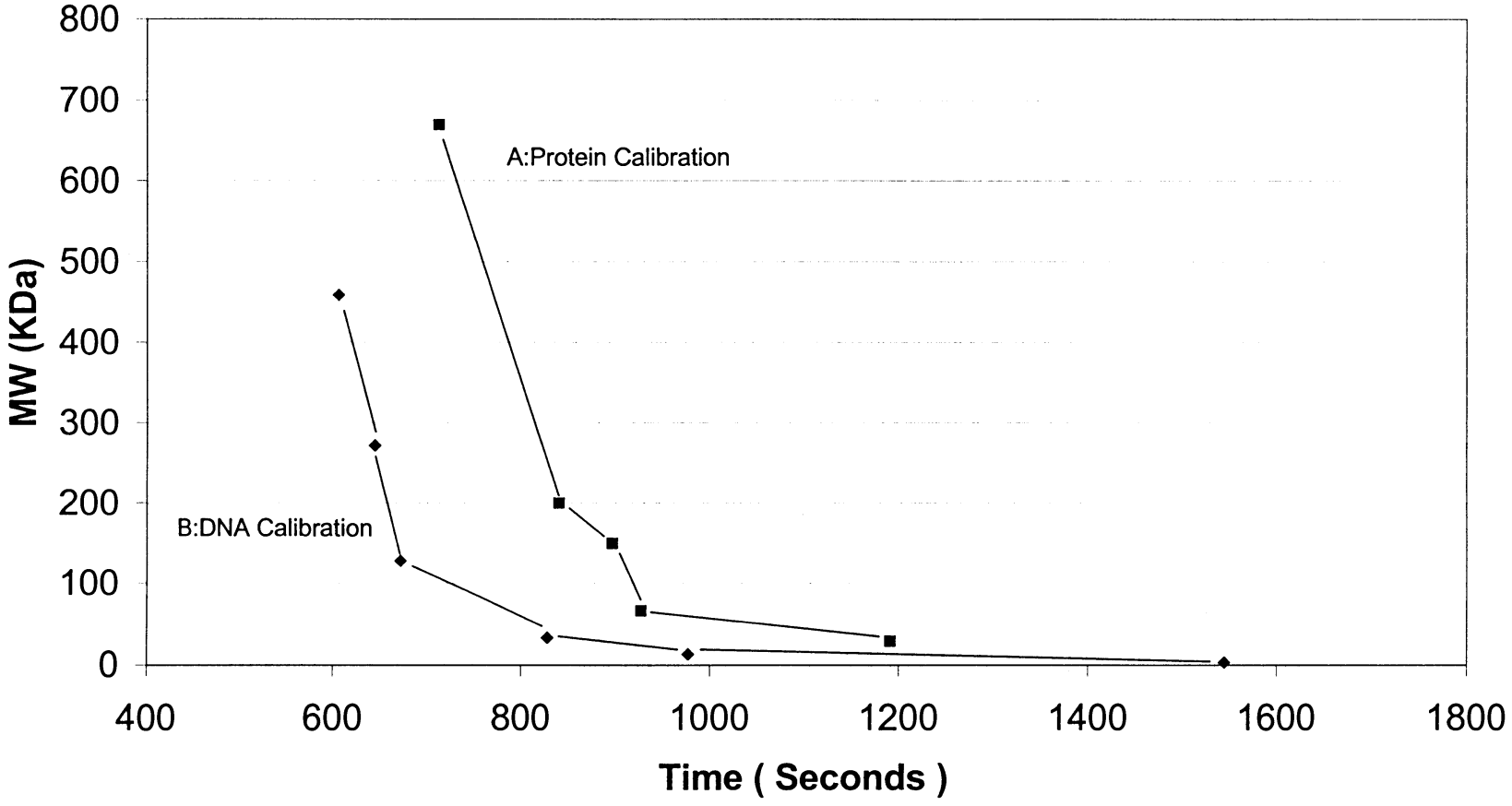

Fig 3 Contrast of DNA calibration and protein calibration (based on 1 bp of DNA weights 660 Da)

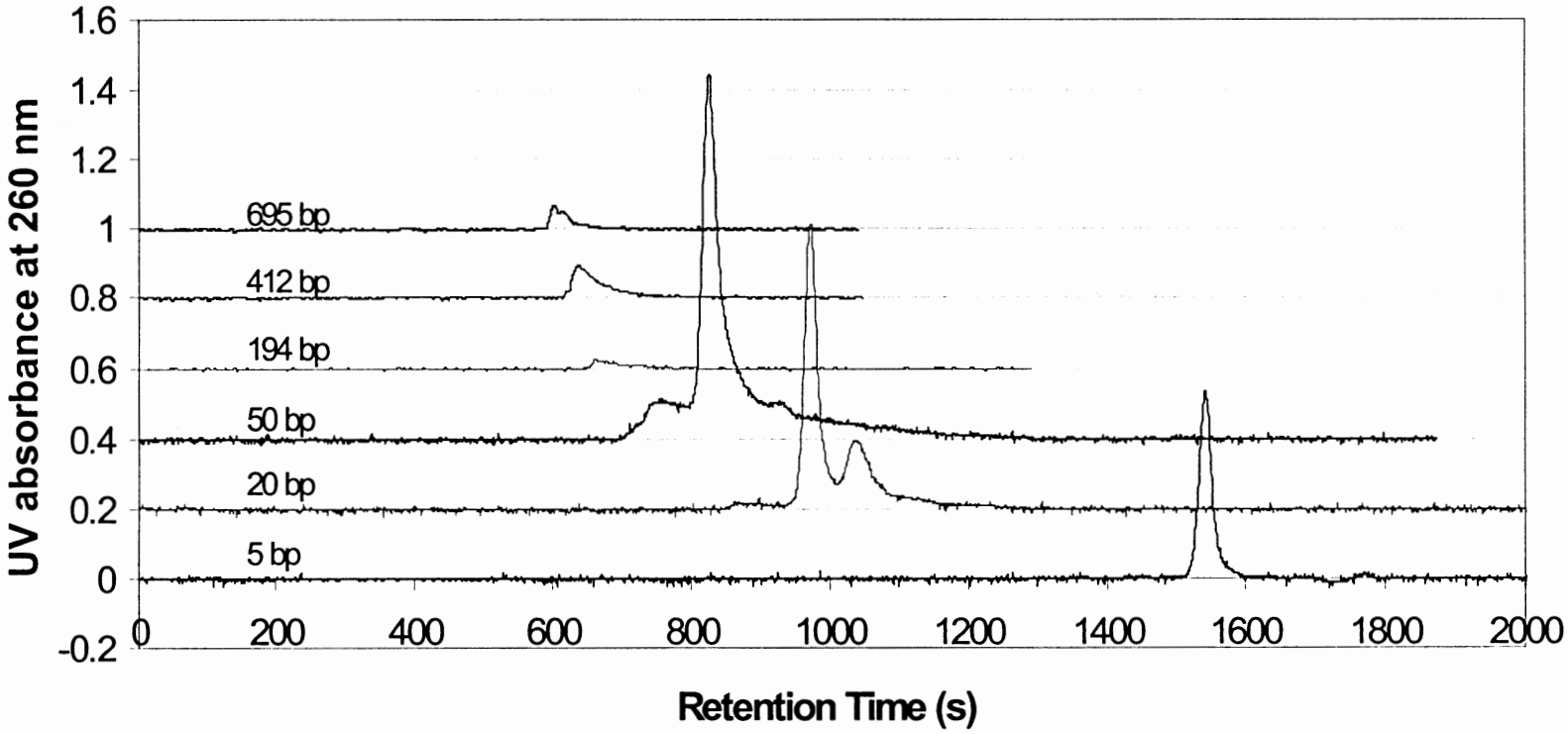

Fig 4 Chromatography of DNA markers

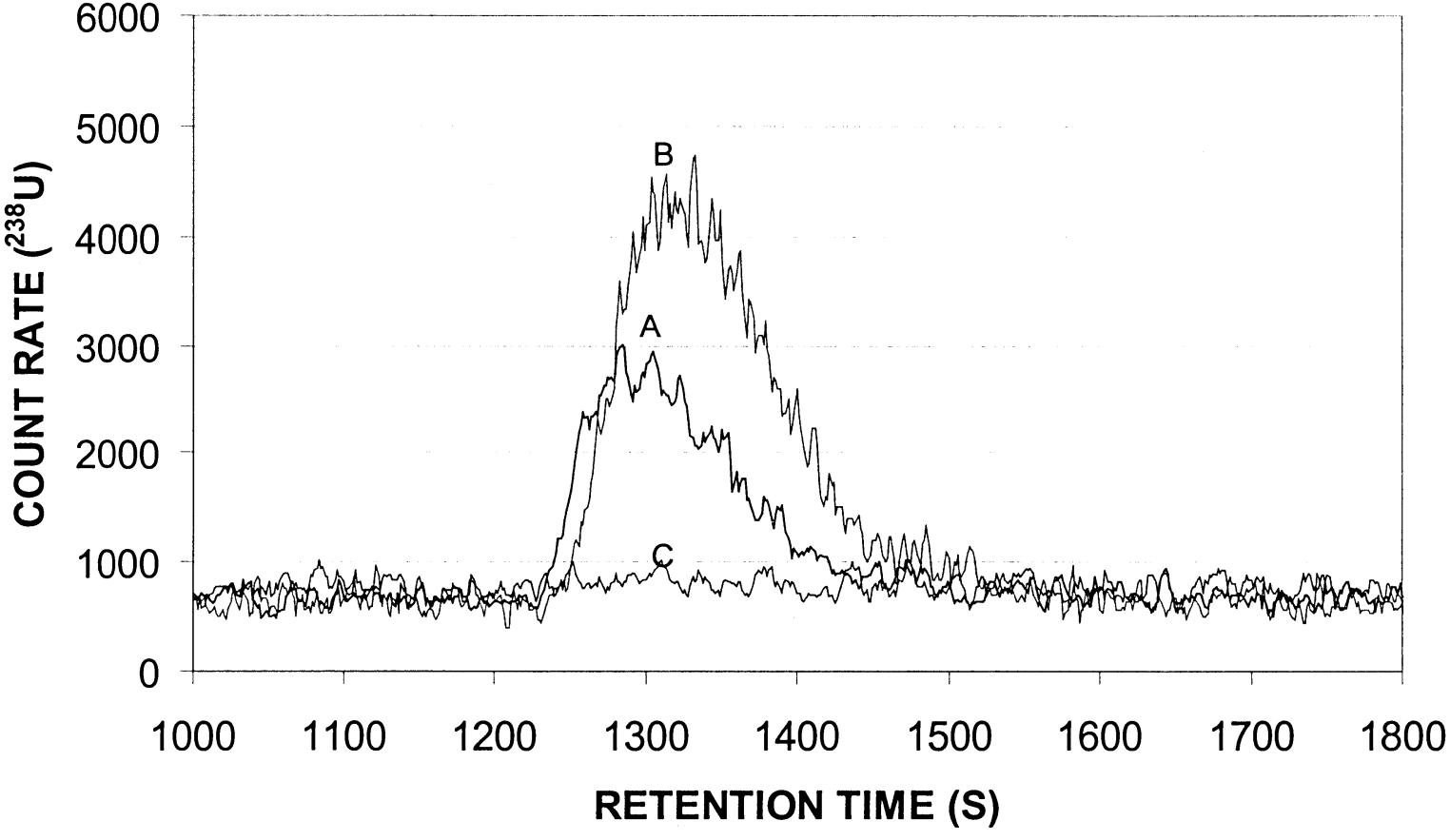

Fig 5A 5 ppm DNA mixture

A: + 1ppb U after 0.5 hr, B: + 1 ppb U after 4.5 hrs, C: DNA alone

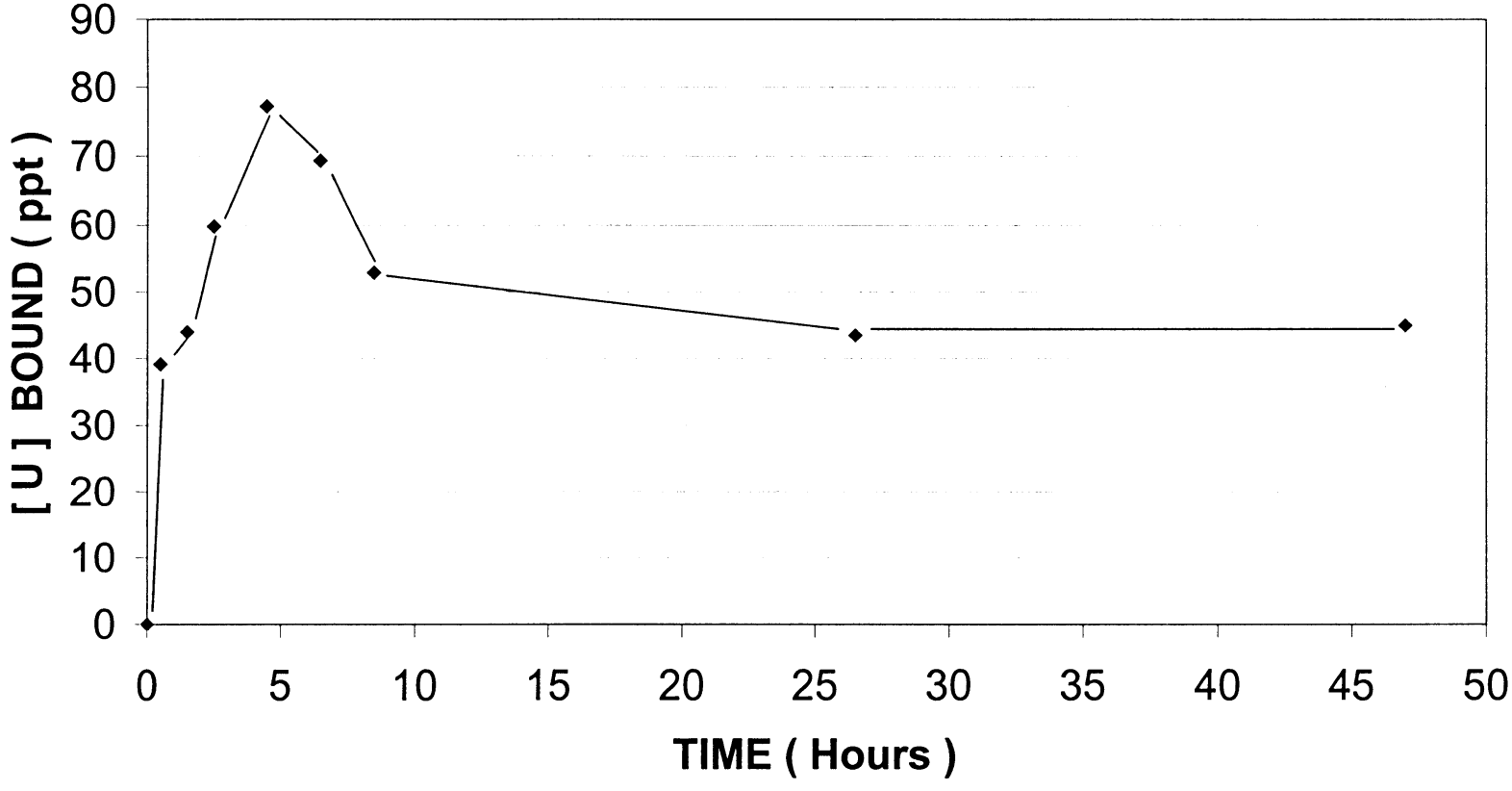

Fig 5B Bonding curve of 5 ppm DNA mixture spiked with1ppb U

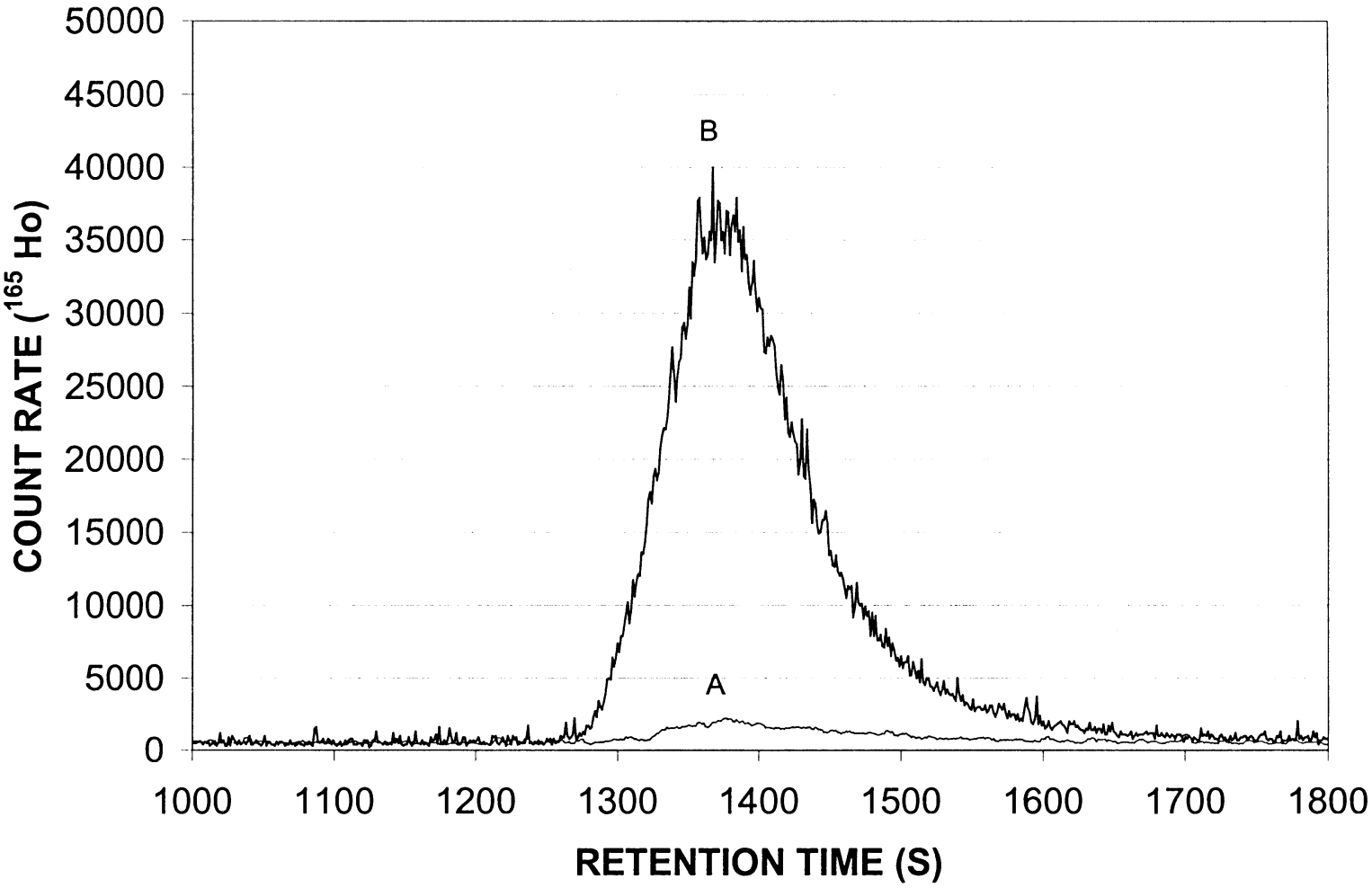

Fig 6A A: 5 ppm DNA mixture alone, B: 5 ppm DNA mixture + 1 ppb Ho after 10 mins

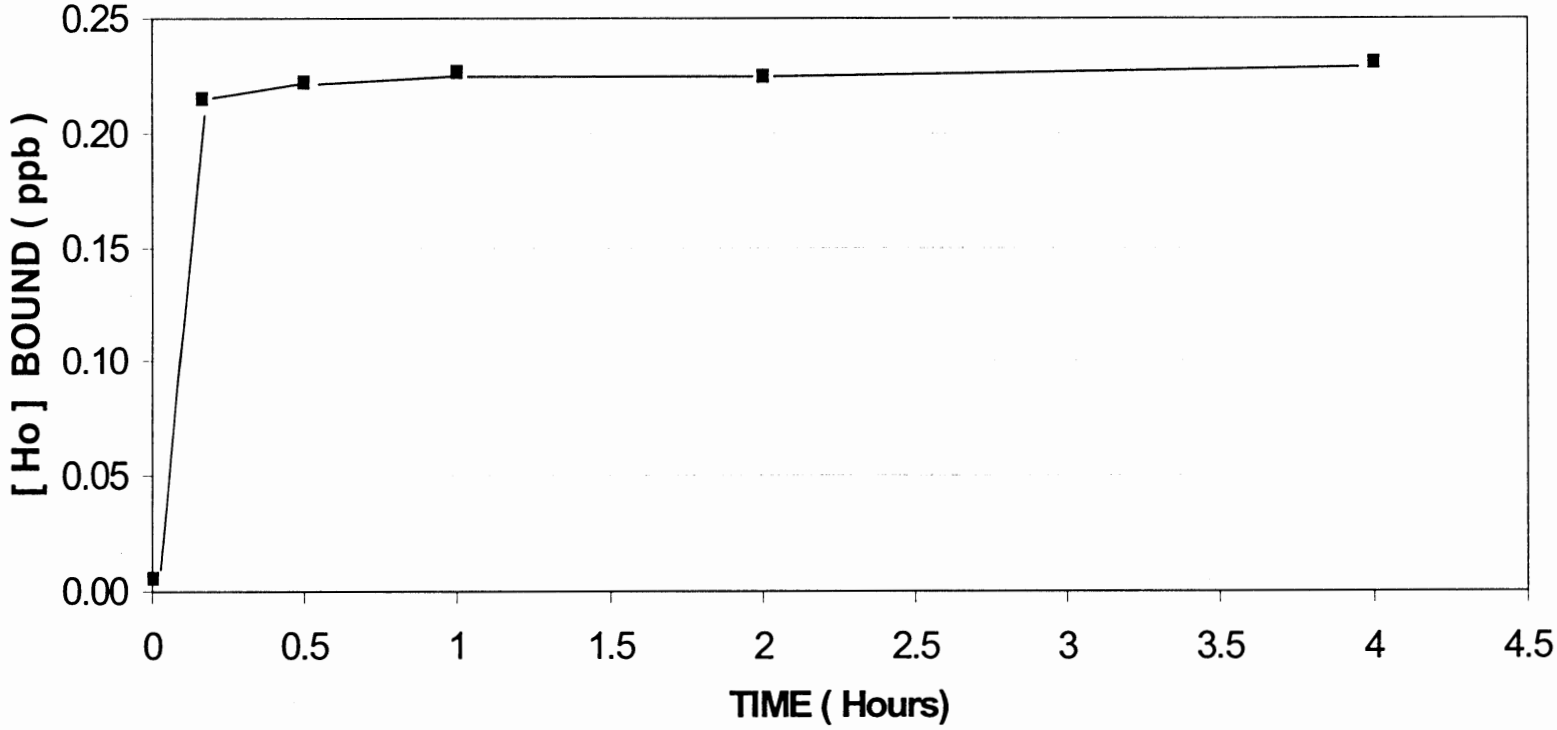

Fig 6B Bonding curve of 5 ppm DNA mixture spiked with 0.5 ppb Ho

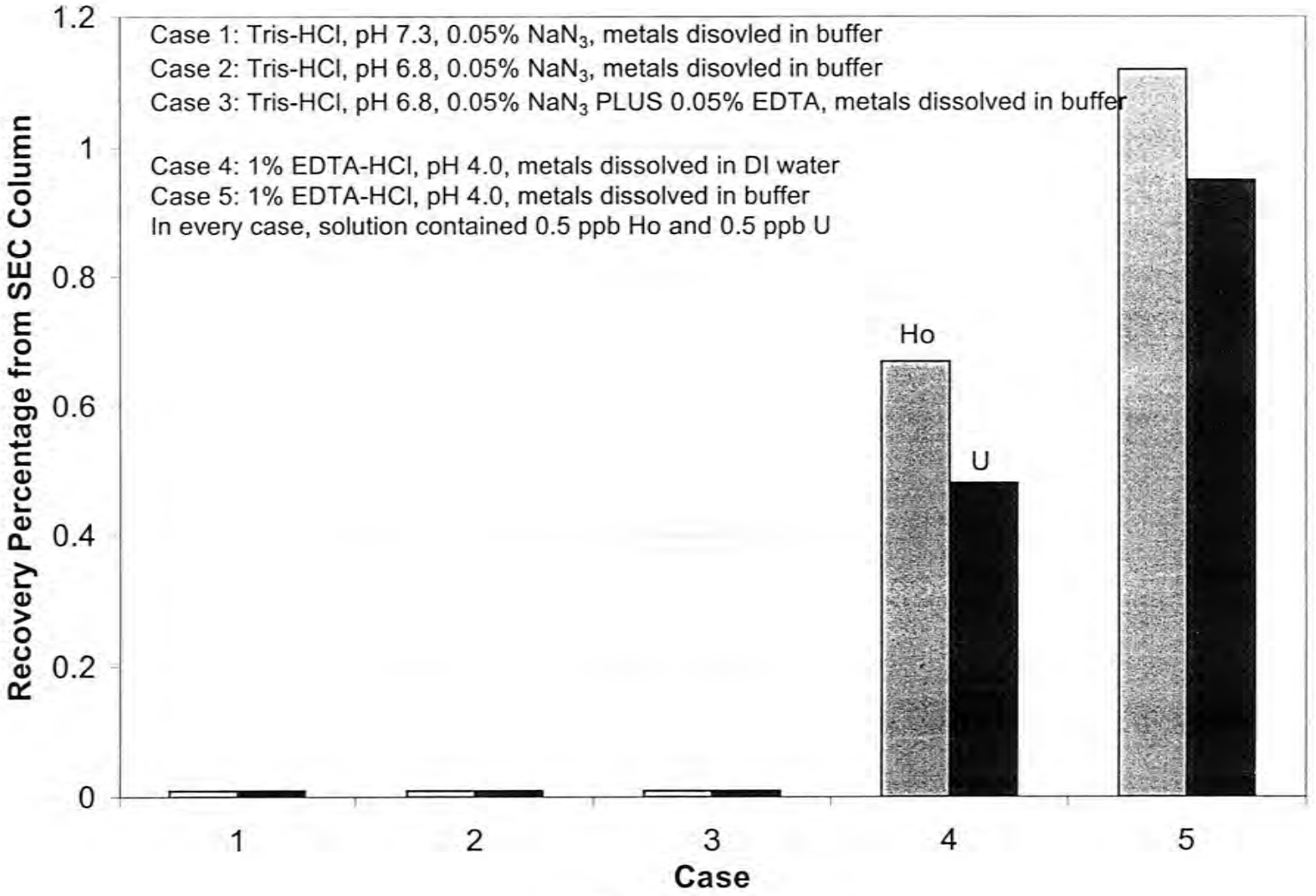

Fig 7A Metal Recovery Chart

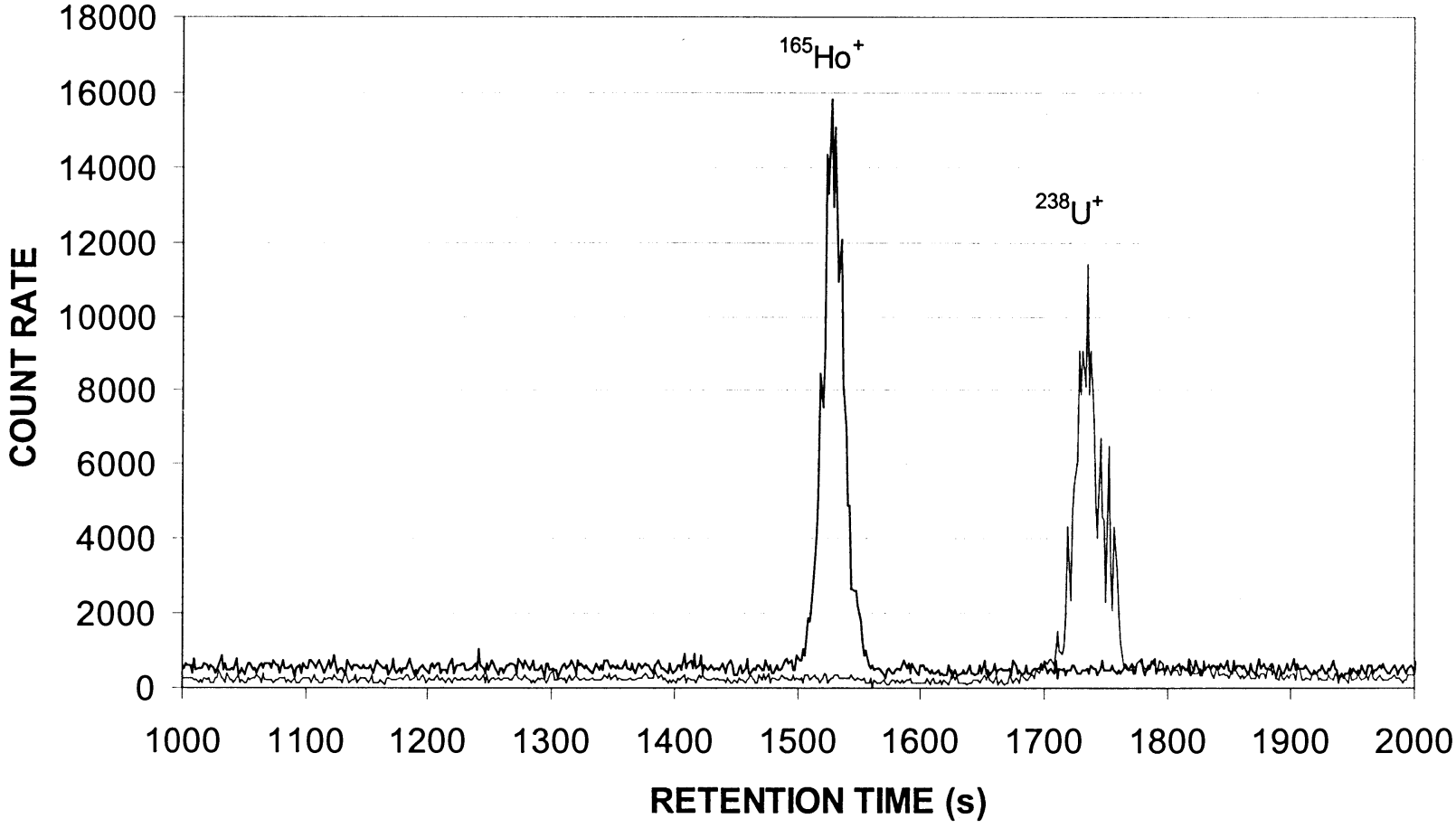

Fig 7B 1% EDTA-HCl, pH 4.0, 0.5 ppb U and Ho Dissolved in buffer

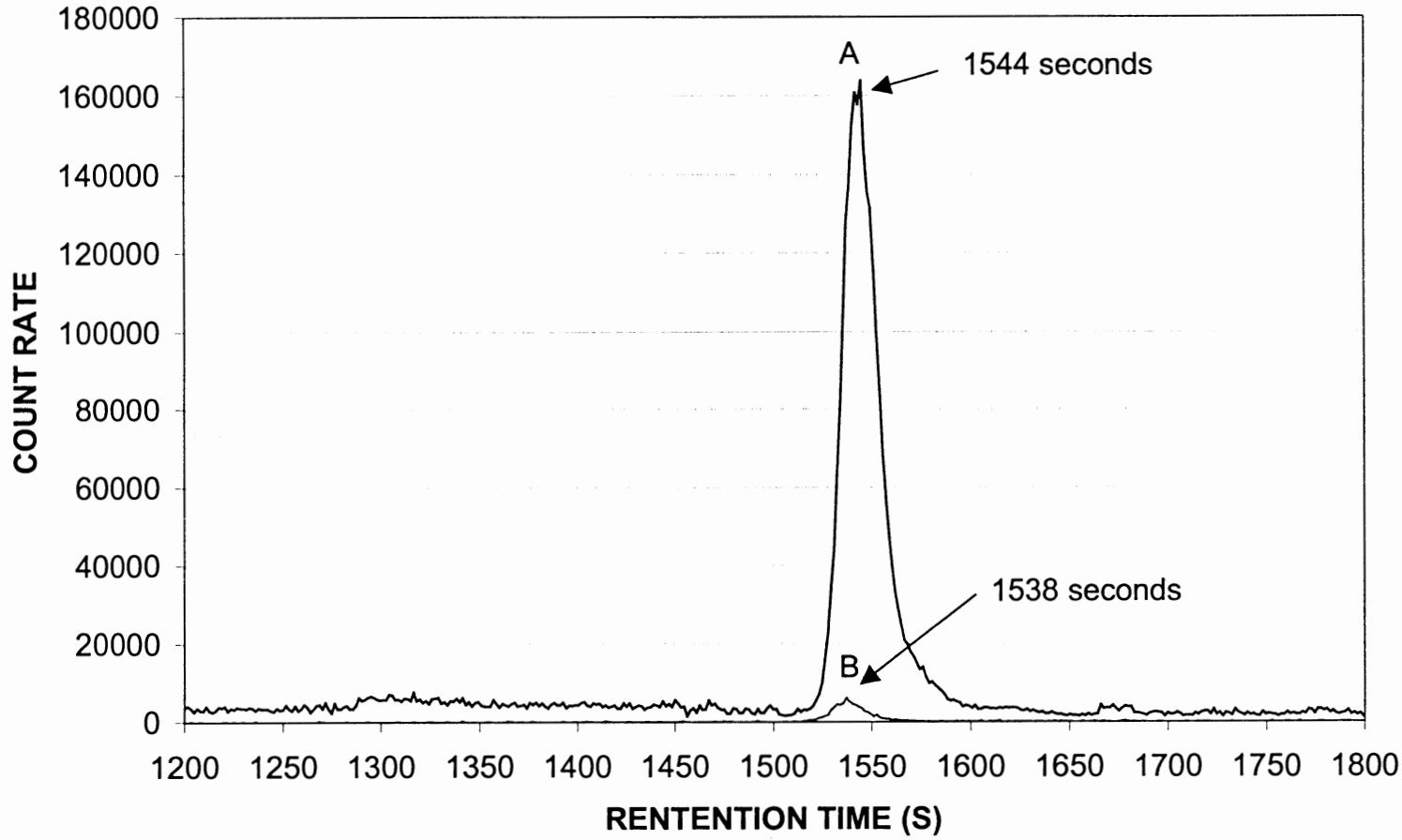

Fig 8A Medium resolution, 1 ppb uranium spiked to 50 ppm DNA fragment of 5 bp
A: signal of $^{31}P^{+}$, B: signal of $^{238}U^{+}$

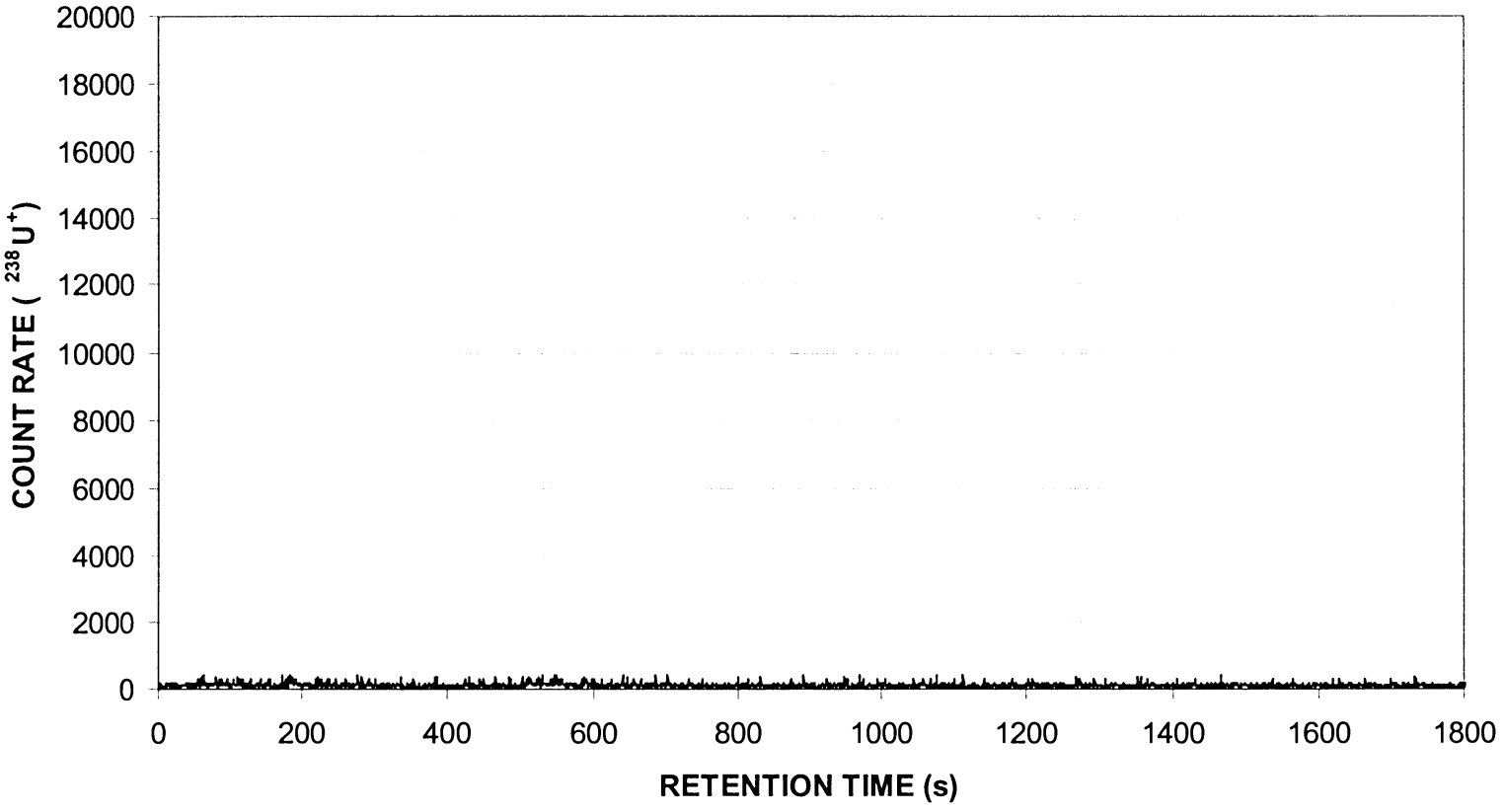

Fig 8B 0.5 ppb uranium spiked to 20 bp DNA fragment

3. QUANTIFICATION OF PHOSPHOROUS IN PROTEINS BY INDUCTIVELY COUPLED PLASMA MASS SPECTROMETRY USING INORGANIC PHOSPHOROUS STANDARDS

Yongjin Hou and R. S. Houk

A paper to be submitted to Journal of Analytical Atomic Spectrometry

ABSTRACT

Quantification of phosphorous in proteins is very important to research regarding protein phosphorylation and dephosphorylation. Current methods, however, can not get this work done reliably. The present work showed the possibility of quantifying phosphorus in proteins by using inductively coupled plasma mass spectrometry (ICP-MS) with inorganic phosphorous standards. The detection limit, reliability and accuracy of our new method were evaluated and tested with phosvitin and ß-casein.

INTRODUCTION

Protein phosphorylation and dephosphorylation play significant regulatory roles in a variety of cellular processes such as normal and abnormal cell growth, cell death, and secretion. While non-covalent (i.e. allosteric) regulation of proteins serves mainly a homeostatic function, protein phosphorylation is more concerned with switching of cellular activity from one state to another. Phosphorylation appears to have two main functions: 1. It is the major mechanism by which cells respond to extracellular signals such as hormones and growth factors. 2. It is responsible for the timing of events which must occur at defined stages in the

cell cycle, such as DNA synthesis and mitosis [1]. As a result, detecting changes in the phosphorylation status of proteins is becoming increasingly important.

Present methods, however, can not detect or quantify phosphorous in proteins very well. One of present approaches is to artificially incorporate $^{32}PO_4^{3-}$ into the cellular ATP pool and then measure the densitometry of autoradiographs. This kind of operation requires the use of 1-10 mCi of ^{32}P, significantly more than what is used in most experiments so the radioactivity of ^{32}P is a concern [1]. Since ^{32}P-labeling brings additional phosphorous to proteins and what is measured is the extra radioactive phosphorous bound to protein, the measurements may not reflect the natural status of phosphorylation. Furthermore, ^{32}P-labeling is not suitable for most applications in plant biology. The second approach is immunodetection with antibodies against phoshorylated amino acids. As we know, the immunoreaction is amino acid specific which means for phosphorous on certain amino acid, a specific antibody has to be used. In different proteins, the reactivity may vary greatly. The third approach is to hydrolyze phosphate groups of phosphoprotein and then let the free phosphate group react with Ca^{2+} or some other reagents for analysis. The reactivity again depends greatly on the surroundings. Fourth, electrospray ionization mass spectrometry (ESI-MS) and matrix assisted laser desorption ionization mass spectrometry (MALDI-MS) can be used to locate sites of phosphorylation but they are not suitable for quantification either because phosphorous in proteins can not be equally or quantitatively ionized in the two soft ionization sources.

With current methods, the only way to reliably quantify phosphorous of a protein, is to find the same protein or at least a very similar protein as the standard under the condition that the amount of phosphorous in the protein standard is known. Apparently, this is difficult

because in real research, the information regarding proteins may be unclear and it may be very difficult to find its phosphorylation standard. Recently saw a paper, which utilized ICP-MS for detecting phosphorous in peptides (MW < 4 kDa) but no quantification was mentioned in that work [2].

In our work, ICP-MS was employed to quantify phosphorous in proteins by detecting ^{31}P which is the only natural isotope. Though for ICP, phosphorous is a hard element, only 10 % of which can be ionized around 7000 K and $n_e = 1.5 \times 10^{15}$ cm^{-3} , ICP is still the most thorough source to convert phosphorous into atomic ions. Detecting $^{31}P^+$ with ICP-MS requires removal of spectral interference, such as NOH^+. Our magnetic sector instrument can provide resolution of 4000 and even higher (10 % valley) so phosphorous can be confidently distinguished from interference. We tried an inorganic compound, NaH_2PO_4 as phosphorous standard to quantify phosphorous in proteins. If this could work, there would be less need of protein standard with known amount of phosphorylation.

Since proteins are much bigger molecules than NaH_2PO_4, the reliability and accuracy of quantifying phosphorous in proteins with inorganic compound are largely based on the extent of atomization and ionization for proteins in ICP, relative to the corresponding processes for inorganic phosphate. This issue was investigated first in our present work. The improvement of the detection limit for phosphorous was mainly explored in two ways. First, organic modifiers were added to DI water and compared in the terms of blank level, blank noise, sensitivity and finally detection limit. As claimed by several researchers, organic modifiers can improve the sensitivity of many elements whose ionization energies are between 9 and 11 eV, like phosphorous, 10.48 eV [3-6]. Second, we tried a graphite injector, which was inserted half the way into the plasma. As reported by Clemons et. al., the graphite

injector improved absolute sensitivities of hard-to-ionize elements, such as As, Zn and so on and suppressed MO^+ ions [7]. Phosvitin and β-casein were taken for evaluating the accuracy and reliability of our method because the phosphorous content for these two proteins, is thought to be well understood. The ultimate goal of our research is to quantify phosphorous in proteins or in pharmaceutical compounds by ICP-MS using inorganic phosphorous standard.

EXPERIMENTAL

Instrumentation

The Finnigan Element ICP-MS was the main instrument. The nebulizers used were PFA 100 from Elemental Scientific Inc. and concentric glass nebulizer inserted with silica capillary (246 μm ID, 361 μm OD). The graphite injector consisted of three parts: quartz tube, alumina tube and pyrolytic graphite tube (2 mm i.d. x 5 mm o.d. x 35 mm long). The alumina tube was the connector, one end tightly inserted with quartz tube and the other end with graphite tube. Before use, the graphite tubes were leached in 5% HCl for 8 hrs. The peristaltic pump was Minipulse , Gilson and the syringe pump was 74900 series, from Cole Parmer Instrument Company. The injection valve, 9725 i from Reodyne was originally supplied with 20 μl PEEK loop. The PEEK tubing was replaced with either 10 μl Teflon loop or 10 μl fused silica capillary loop.

Reagents and solutions

High purity HCl was from J. T. Baker Company. Phosphorous solution (21.8 ppb) was prepared from solid NaH_2PO_4, ACS, Fisher Scientific and used as the inorganic standard. ß-casein (Sigma-Aldrich) was lyophilized powder and then it was dissolved in DI

water to become stock solution at 400 ppm in the term of protein. Phosvitin was bought from Pierce Company as 1 mg powder and then it was dissolved in 2 ml DI water to become the other protein stock solution.

Methods

In all experiments, medium resolution ($m/\Delta m = 4000$) was chosen and mass window was set to 150%, peaks to 20, search window to 50% and integration to 80%.

Two data acquisition methods were designed. First one is the spectrum method. In this method, either PFA or glass nebulizer was pumped by peristaltic pump at the rate of 100 μL/min and samples were taken through the pump tubing. Each acquisition consisted of 100 runs and 1 pass, which meant there were 100 spectra totally for each acquisition. In this case, the counts of all peaks at each nominal m/z in each spectrum were added up and then the sums of the 100 spectra were averaged. The averaged sum at each nominal m/z should be proportional to concentration.

The second method is flow injection. In this method, either PFA or glass nebulizer was pumped by a syringe pump at the rate of 100 μL/min and samples were injected through the 10 μl loop of the injection valve. Each acquisition consisted of 300 runs and 1 pass so there were 300 spectra for each acquisition. In this case, the counts of all peaks at each nominal m/z in each spectrum were also summed but we didn't average the sums. Instead, the sum of each spectrum was plotted verse time to generate a chromatogram.

In our experiments, combinations of nebulizers (PFA or glass), methods (spectrum or flow injection) and torches (normal or graphite injector) were made according to need. The details are listed in Table 1.

RESULTS AND DISCUSSION

Aerosol gas flow rate plots

In this measurement, the signals of $^{31}P^+$, $^{31}P^{16}O^+$, $^{31}P^{16}O_2^+$, $^{31}P^{16}O_3^+$, $^{31}P^{16}O_4^+$ were measured at different aerosol flow rates for the inorganic standard and ß-casein as well. Both normal torch and graphite injector were tried. The maximum aerosol flow rate was 1.2 L/min, limited by the geometry of the PFA 100.

As shown in Fig 1A and Fig 1B, the optimum aerosol flow rates for detecting $^{31}P^+$of inorganic phosphate and of ß-casein were the same. In both Figures, at the optimum flow rate, not only $^{31}P^+$ signal reached its maximum but also the ratios of phosphorous to its oxides were maximized. These observations show that the protein was atomized and ionized at same position in ICP as inorganic phosphate was.

As shown in Fig 1C and Fig 1D, with the graphite injector, protein and inorganic compound still share the same best aerosol flow rate. It was noticeable, however, this flow rate was shifted to a smaller value compared with that of normal torch. With the graphite injector, the signals of phosphorous oxides from the aerosol were appreciably depressed. All those observations were consistent with previous research on graphite injector [7].

Quantification of phosphorous in phosvitin

Four phosvitin solutions were 32 ppb, 160 ppb, 800 ppb and 4 ppm in the term of phosvitin. The reported weight percentage of phosphorous of phosvtin ranged from 9.6% to 10.4% [8, 9]. 10% was taken for our calculations.

As shown in Table 2 and Fig 2A through Fig 2C, the measured phosphorous of phosvitin was close to calculated values. If phosvitin molecules were not introduced, dissociated satisfactorily in ICP or the phosphorous of phosvitin was not ionized to a similar

extent as inorganic phosphorous, then phosvitin wouldn't give close $^{31}P^{+}$ result relative to inorganic phosphorous standard. Thus, $^{31}P^{+}$ is produced with similar efficiency from phosvitin as from inorganic phosphate.

Quantification of phosphorous in ß-casein

Phosphorous in ß-casein was determined with inorganic phosphorous standard by three different approaches. The molecular weight of ß-casein ranges from 23, 944 to 24,092 Da and each ß-casein contains 4 to 5 phosphate residues [10-12]. In our calculations, the MW of ß-casein was rounded to 24 kDa and each protein molecule was supposed to contain 4.5 phosphate residues. So the weight percentage of phosphorous in ß-casein was 31 Da x 4.5 /24 kDa = 0.58 %.

As shown in the first three columns of Table 3, spectrum method didn't give good results where the measured values were off from calculated values and the ratios increased with protein concentration. This indicated that ß-casein stuck to the tubing of peristaltic pump. The results in the next three columns from the flow injection method plus glass nebulizer had the same problem, which meant ß-casein could also be retained by the silica capillary tubing. The ratios in the last three columns didn't change very much, which showed that the sticking effect was less severe with Teflon material. Based on the results of the last three columns, Line B of Fig 2A was plotted, in which the basic trend was a linear line but the measured values was just about half of those expected. Two reasons, in our opinion, were probably responsible for the discrepancy. First, ß-casein could still stick to the Teflon uptake line even though the linearity was maintained. Second, our ß-casein sample might not have as much phosphorous as thought.

Fig 3A and Fig 3B are two examples of flow injection, one from inorganic standard and the other one from ß-casein. To make accurate calculations, the baseline needs to be subtracted from peaks so that net peak areas can be obtained, and it is not the peak height but the net peak area that is really proportional to concentration. The concentration of phosphorous in Fig 3B was determined by measuring the ratio of averaged net peak area of Fig 3B over averaged net peak area of Fig 3A since the concentration of phosphorous in the inorganic standard was known to be 21.8 ppb.

Rinse-out curve

150 ppb inorganic phosphorous was compared with phosvitin and ß-casein whose calculated concentrations in the term of phosphorous were both 150 ppb. All three solutions were dissolved in DI water. It must be pointed out, in this experiment, data were acquired by the flow-injection method but samples were taken by natural uptake of Teflon tubing without any pump or going through any injection valve.

As shown in Fig 4A and Fig 4B, the rising edge and falling edge of the peak for ß-casein were as sharp as those for phosvitin and inorganic phosphate. Thus, none of these species stuck to the Teflon tubing longer than the others. During the 20 seconds or so when the samples were introduced, the signals were not very stable. This was because after being used for a long time, the tiny capillary tubing of Teflon nebulizer could be clogged partly by particles in samples, so that the uptake rate changed. Cleaning the Teflon with 5% HNO_3 or 2% HF and using a pump could improve the signal stability appreciably.

If the stickiness was not the reason why just half amount of phosphorous of ß-casein as predicted was measured, then it was much more likely that the ß-casein in our experiments

didn't have as much as phosphorous as thought. We suspects ß-casein lost its phosphorous through hydrolysis during purification.

Detection limit comparison

21.8 ppb inorganic phosphorous standard was used for evaluation. With normal torch plus PFA nebulizer, solvent effects on detection limit were compared. As listed in Table 4, the absolute sensitivity in 3 % MeOH was about 40 % higher than that in DI water. Triethanolamine at 6 % generated almost 1.8 times sensitivity of DI. However, DI water had the lowest blank level and noise standard deviation and ultimately its detection limit for phosphorous was as good as that of 3% MeOH. The detection limit with 6 % triethanolamine was worse due to its high, noisy blank level.

In the case of normal torch plus glass nebulizer, detection limit was not good, due to the increased blank and decreased sensitivity.

The spectrum method with DI water as solvent produced detection limit of 0.08 ppb. If this method took 1 min or in another word, 100 µL sample, then the absolute detection limit was 0.08 ppb x 100 µl = 0.08 ng/ml x 0.1 ml = 0.008 ng = 8 pg phosphorous.

Flow injection method required only 10 µL sample but the detection limit couldn't be as low as 0.08 ppb since we were unable to improve the standard deviation by averaging spectra. In this case, the detection limit was around 2 ppb or 2 ppb x 10 µl = 2 ng/ml x 0.01 ml = 0.02 ng = 20 pg phosphorous.

We believe, in a clean laboratory environment, the blank level and blank standard deviation would be decreased further so that the detection limit for phosphorous can be improved further.

CONCLUSION

The overall conclusion is phosphorous in proteins can be quantified in ICP-MS with inorganic phosphorous standard and meanwhile the accuracy, reliability and detection limit are very good. The conclusion may be specified as follows:

1. Protein requires the same optimum aerosol flow rate as inorganic phosphate so the dissociation and atomization of protein in ICP is not a problem.

2. There is very close match between measured values and calculated values for phosvitin. It means proteins can be introduced, atomized and ionized to the same degree as inorganic phosphate is. So inorganic phosphate can be used as standard to quantify phosphorous in proteins, at least phosvitin.

3. The measured phosphorous concentrations in ß-casein were about half of those expected. The possibility of protein's sticking to Teflon can be ruled out since the rising edge and falling edge of peaks for ß-casein are just same as those for phosvitin and inorganic phosphate. So we doubt if the ß-casein in our experiments had as much phosphorous as thought. Hydrolysis may be the reason of less phosphorous being present.

4. For phosphorous, the detection limit can be as good as 8 pg with spectrum method or 20 pg with flow injection method. The organic modifier improves sensitivity by 40 % to 80 % but can not improve detection limit due to increased blank.

ACKNOWLEDGEMENTS

Ames Laboratory is operated for U.S. Department of Energy by Iowa State University under Contract No. W-7405-ENG-82. The authors wish to thank Dr. Chitinis and his student, Maria Pantelidou, who both are in plant science for financial support.

REFERENCES

1. D. G. Hardie, *Protein Phosphorylation, A Practical Approach*, Oxford University Press, 1993.
2. Mathias Wind, Michael Edler, Norbert Jakubowski, Michael Linscheid, Horst Wesch and Wolf D. Lehmann, *Anal. Chem.*, 2001, **73**, 29.
3. S. C. K. Shum, S. K. Johnson, H. Pang and R. S. Houk, *Appl. Spectrosc.*, 1993, **47**, 575.
4. Shuqin Cao, Hangting Chen and Xianjin Zeng, *J. Anal. Atomic Spectrom.*, 1999, **14**, 1183.
5. Erik H. Larsen and Stefan Sturup, *J. Anal. Atomic Spectrom.*, 1994, **9**, 1099.
6. Leon Pszonicki and Jakub Dudek, *J. Anal. Atomic Spectrom.,*, 1999, **14**, 1755.
7. P. Scott Clemons, Michael G. Minnich and R. S. Houk, *Anal. Chem.*, 1995, **67**, 1929.
8. Samuel E. Allerton and Gertrude E. Perlmann, *J. Biol. Chem.*, 1965, **240**, 3892.
9. Robert W. Rosenstein and George Taborsky, *Biochemistry,* 1970, **9**, 658.
10. H. W. Modler, *Journal of Dairy Science,* 1985, **68**, 2195.
11. W. N. Eigel, J. E. Butler, C. A. Ernstrom, H. M. Farrell, JR., V. R. Harwalkar, R. Jenness and R. McL. Whitney, *Journal of Dairy Science*, 1984, **67**, 1599.
12. Carole L. Cramer and Rowland H. Davis, *J. Biol. Chem.*, 1984, **259**, 5152.

Table 1 Experiment setup

Experiment	Method	Nebulizer	Torch	Measured Isotopes
1. Aerosol Flow Rate	Spectrum	PFA	1) Normal Torch 2) Graphite Injector	^{31}P, $^{31}P^{16}O$, $^{31}P^{16}O_2$, $^{31}P^{16}O_3$, $^{31}P^{16}O_4$
2. Phosphorous in Phosvitin	Spectrum	PFA	Normal Torch	^{31}P
3. Phosphorous in ß-casein	1) Spectrum 2) Flow Injection 3) Flow Injection	1) PFA 2) Glass 3) PFA	Normal Torch	^{31}P
4. Detection Limit	Spectrum	1) PFA 2) Glass	1) Normal Torch 2) Normal Torch	^{31}P
5. Rinse-out Curve	Flow Injection	PFA	Normal Torch	^{31}P

Table 2 Phosvitin (MW: 40 kDa, 10 wt. %)

Phosvitin	Phosphorous of Phosvitin		
Concentration (ppb)	Calculated (ppb)	Measured (ppb)	Ratio (Measured/Calculated)
32	3.2	3.35	1.0
160	16	14.3	0.89
800	80	71	0.89
4000	400	341	0.85

Table 3 β-Casein (MW: 24 kDa, 0.58 wt. %)

Spectrum + PFA			Flow Injection + Glass			Flow Injection + PFA		
Phosphorous			Phosphorous			Phosphorous		
Calculated (ppb)	Measured (ppb)	Ratio	Calculated (ppb)	Measured (ppb)	Ratio	Calculated (ppb)	Measured (ppb)	Ratio
9.28	1.74	0.19	46.4	9.84	0.21	23.2	13.2	0.57
46.4	10.8	0.23	116	33	0.28	58	24.3	0.41
232	96.3	0.42	290	153	0.53	232	132	0.56
			696	955	1.37	464	226	0.48

Table 4 Comparison of detection limits

	Normal Torch + PFA			Normal Torch + glass
Solvent	DI	3% MeOH	6% Triethanolamine	DI
Blank Level of P	1.54×10^3	2.19×10^3	4.92×10^3	5.83×10^3
Blank Noise STD of P	1.31×10^2	1.82×10^2	2.66×10^2	8.33×10^2
Signal of 21.8 ppb P	1.01×10^5	1.42×10^5	1.78×10^5	6.70×10^2
Net signal of 21.8 ppb P	9.97×10^4	1.40×10^5	1.74×10^5	6.12×10^2
Net Signal of 1 ppb P	4.57×10^3	6.41×10^3	7.96×10^3	2.81×10^3
Detection Limit	0.085 ppb	0.085 ppb	0.10 ppb	0.89 ppb

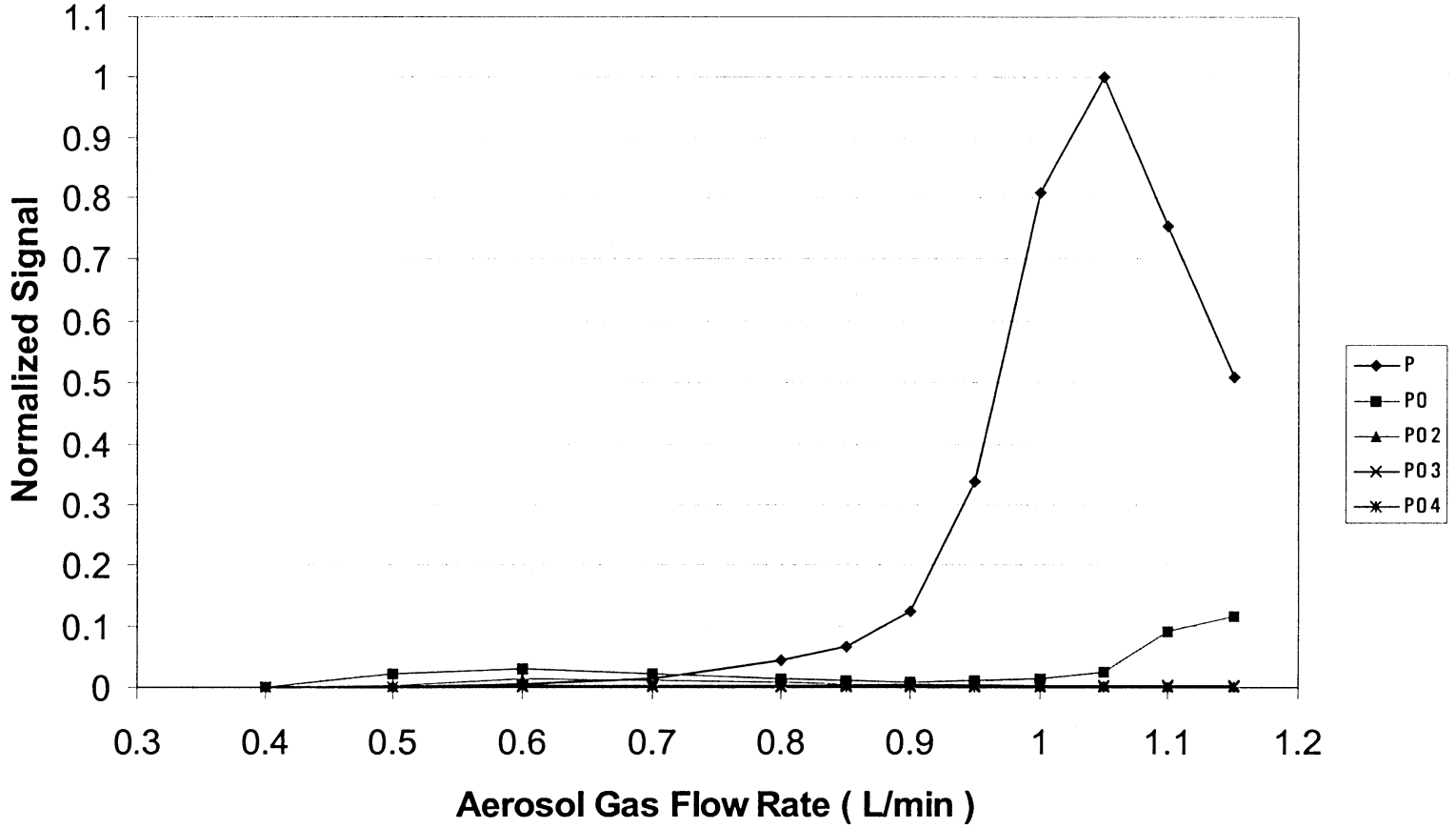

Fig 1A NaH_2PO_4 solution, signals of $^{31}P^+$, $^{31}P^{16}O^+$, $^{31}P^{16}O_2^+$, $^{31}P^{16}O_3^+$, $^{31}P^{16}O_4^+$ at different flow rate

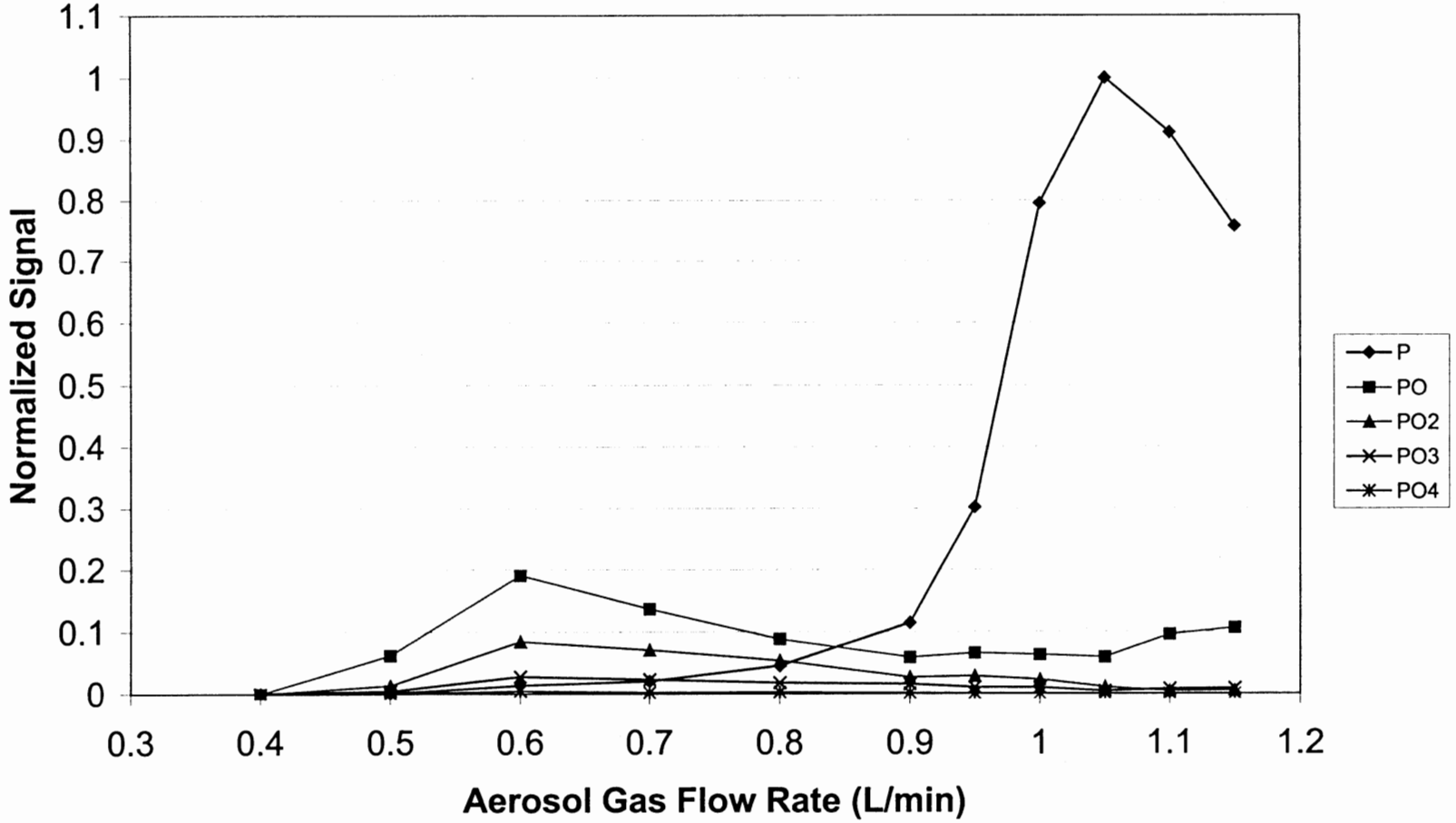

Fig 1B Beta-Casein, signals of $^{31}P^{+}$, $^{31}P^{16}O^{+}$, $^{31}P^{16}O_2^{+}$, $^{31}P^{16}O_3^{+}$, $^{31}P^{16}O_4^{+}$ at different flow rate

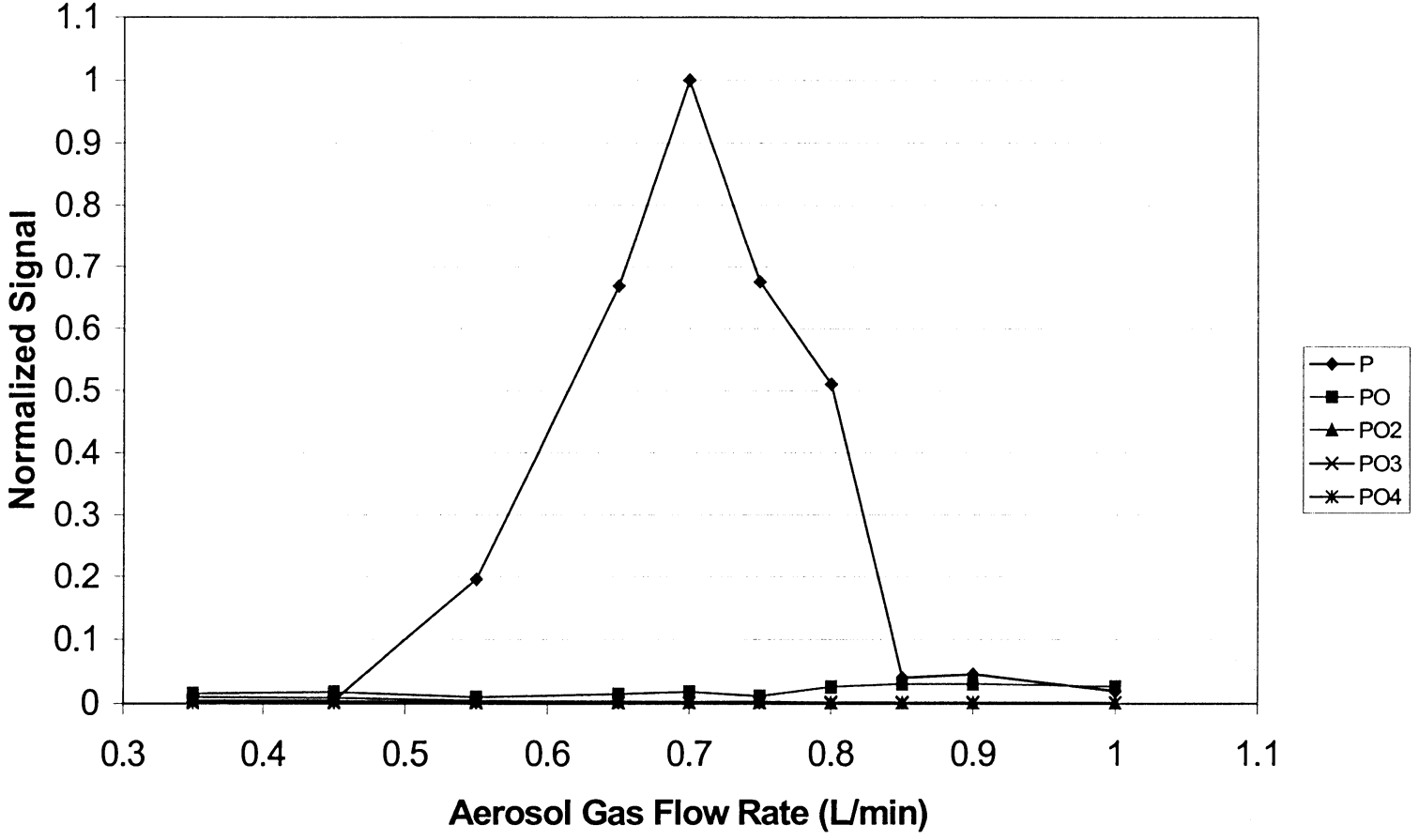

Fig 1C Graphite Injector, NaH_2PO_4, signals of $^{31}P^+$, $^{31}P^{16}O^+$, $^{31}P^{16}O_2^+$, $^{31}P^{16}O_3^+$, $^{31}P^{16}O_4^+$ at different flow rate

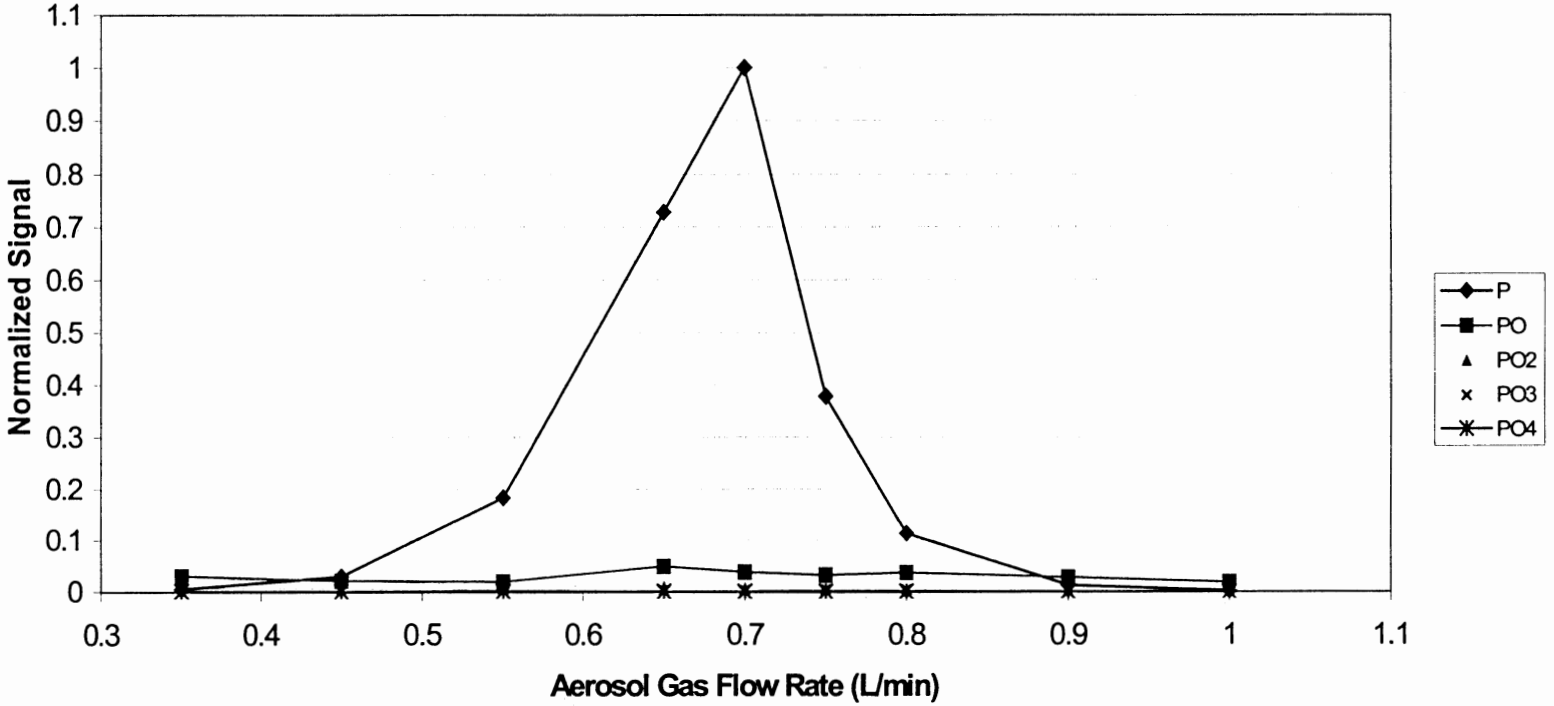

Fig 1D Graphite Injector, Beta-Casein, signals of $^{31}P^{+}$, $^{31}P^{16}O^{+}$, $^{31}P^{16}O_2^{+}$, $^{31}P^{16}O_3^{+}$, $^{31}P^{16}O_4^{+}$ at different flow rate

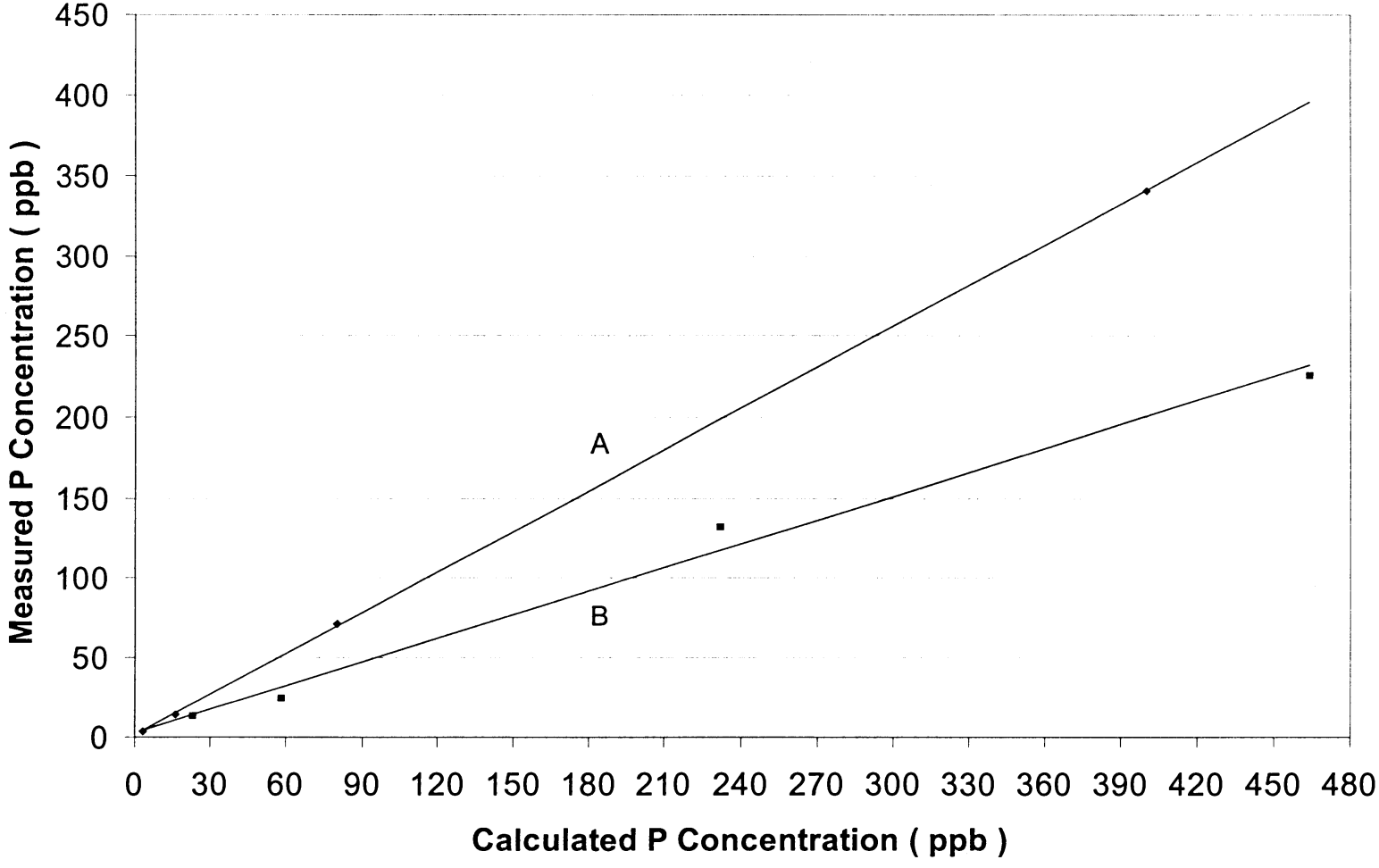

Fig 2A Quantification of phosphorous in proteins
A: Phosvitin, Spectrum Method; B: Beta-Casein, Flow Injection Method

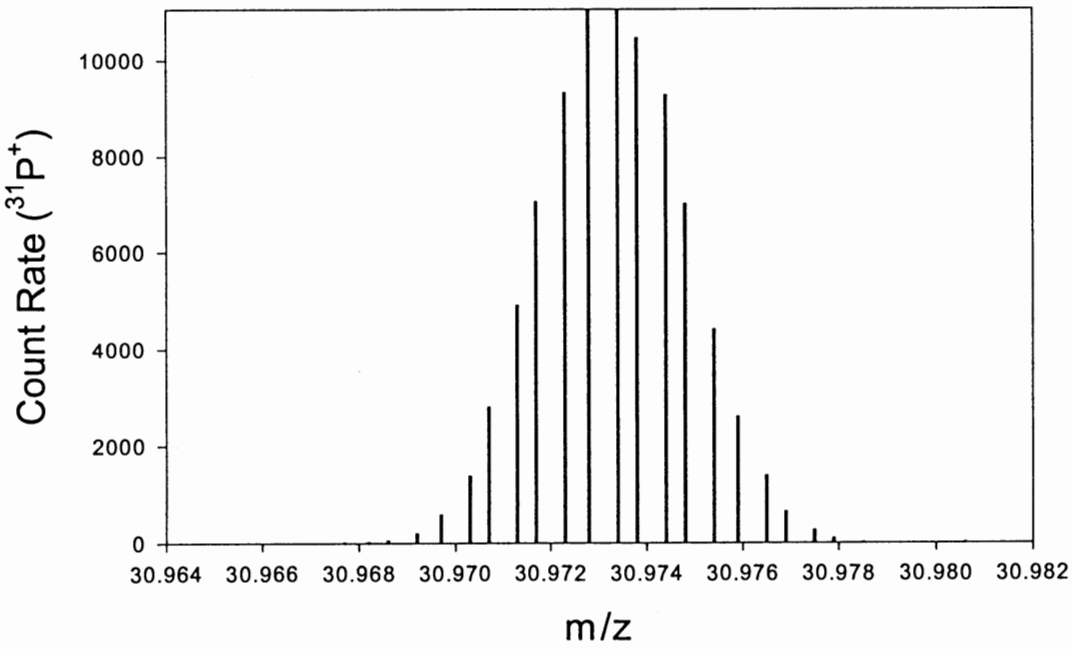

Fig 2B 21.8 ppb phosphorous of NaH_2PO_4

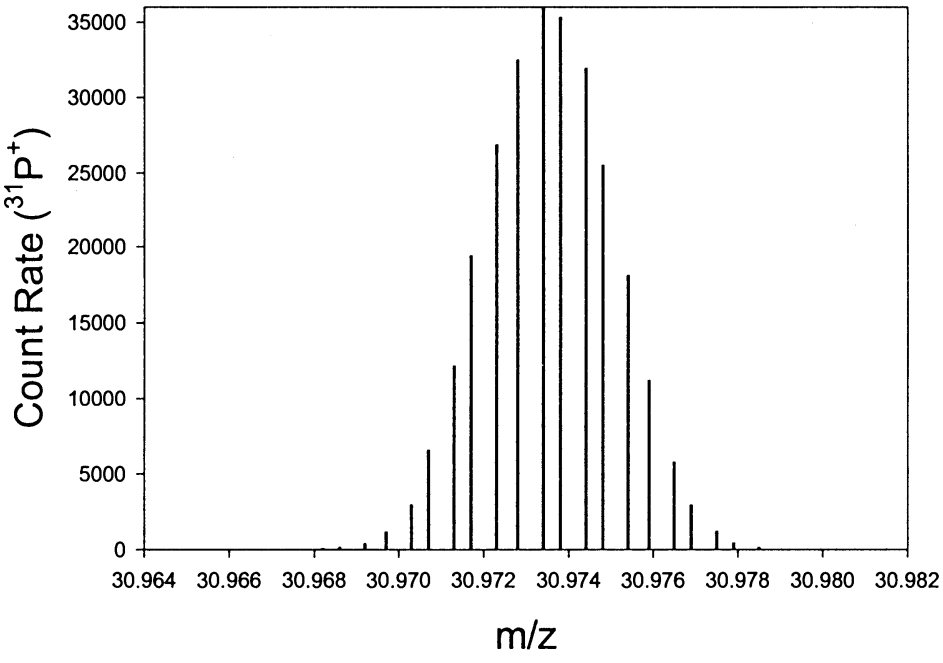

Fig 2C Phosphorous of phosvitin, calculated:80 ppb, measured: 71 ppb

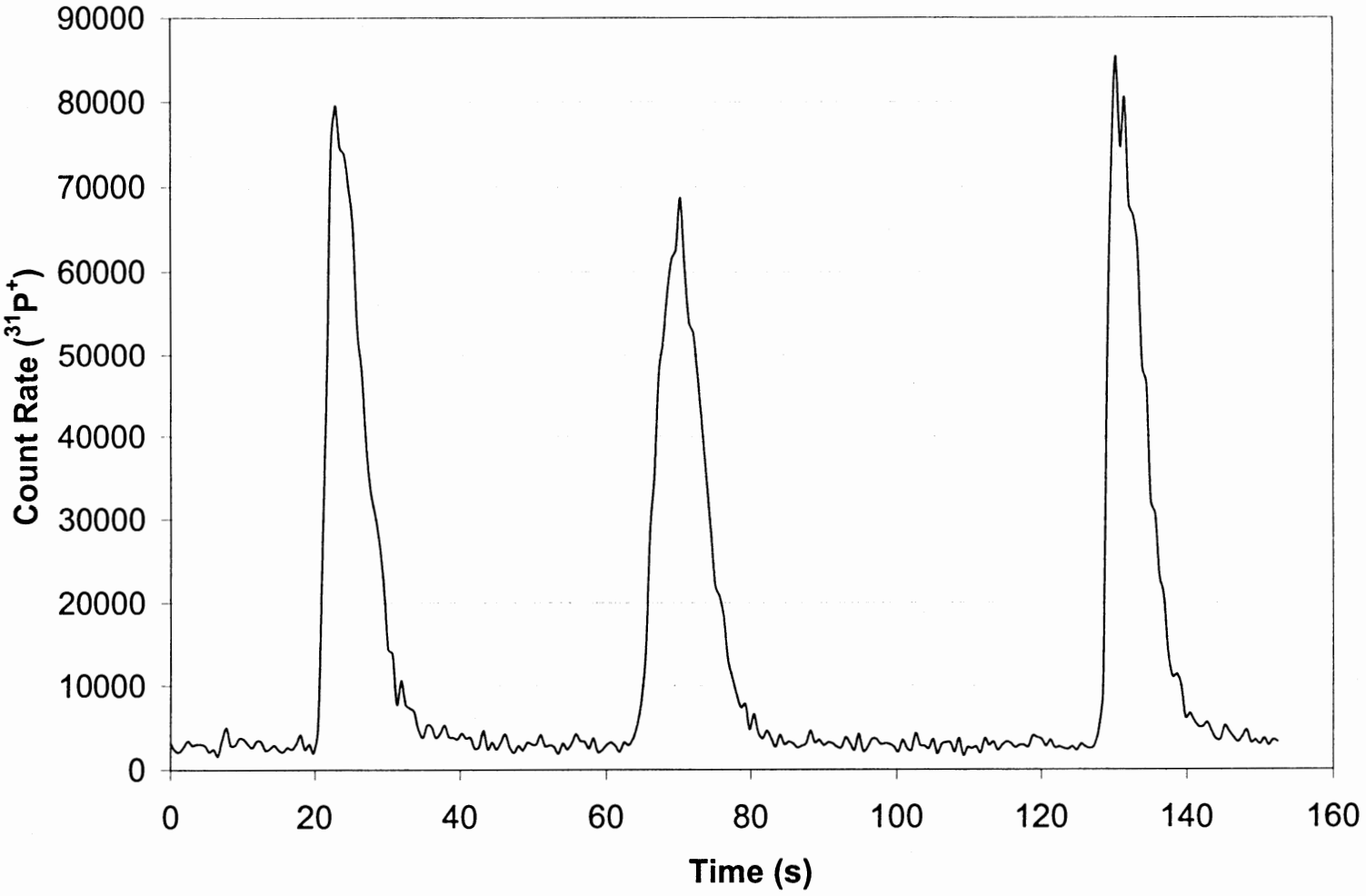

Fig 3A Flow Injection, 21.8 ppb phosphorous in NaH_2PO4

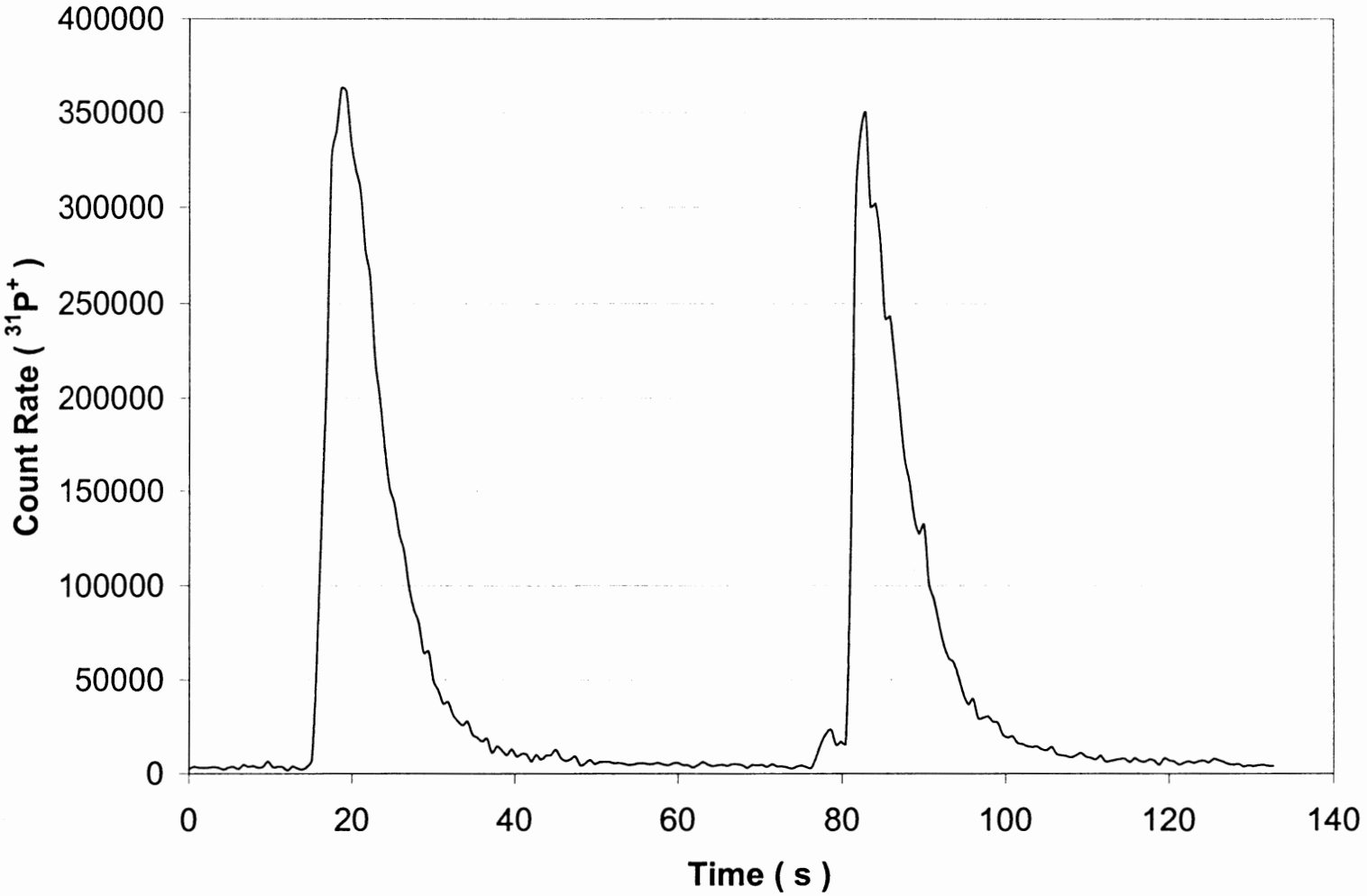

Fig 3B Flow Injection, Phosphorous of beta-casein, Calculated: 232 ppb, Measured: 132 ppb

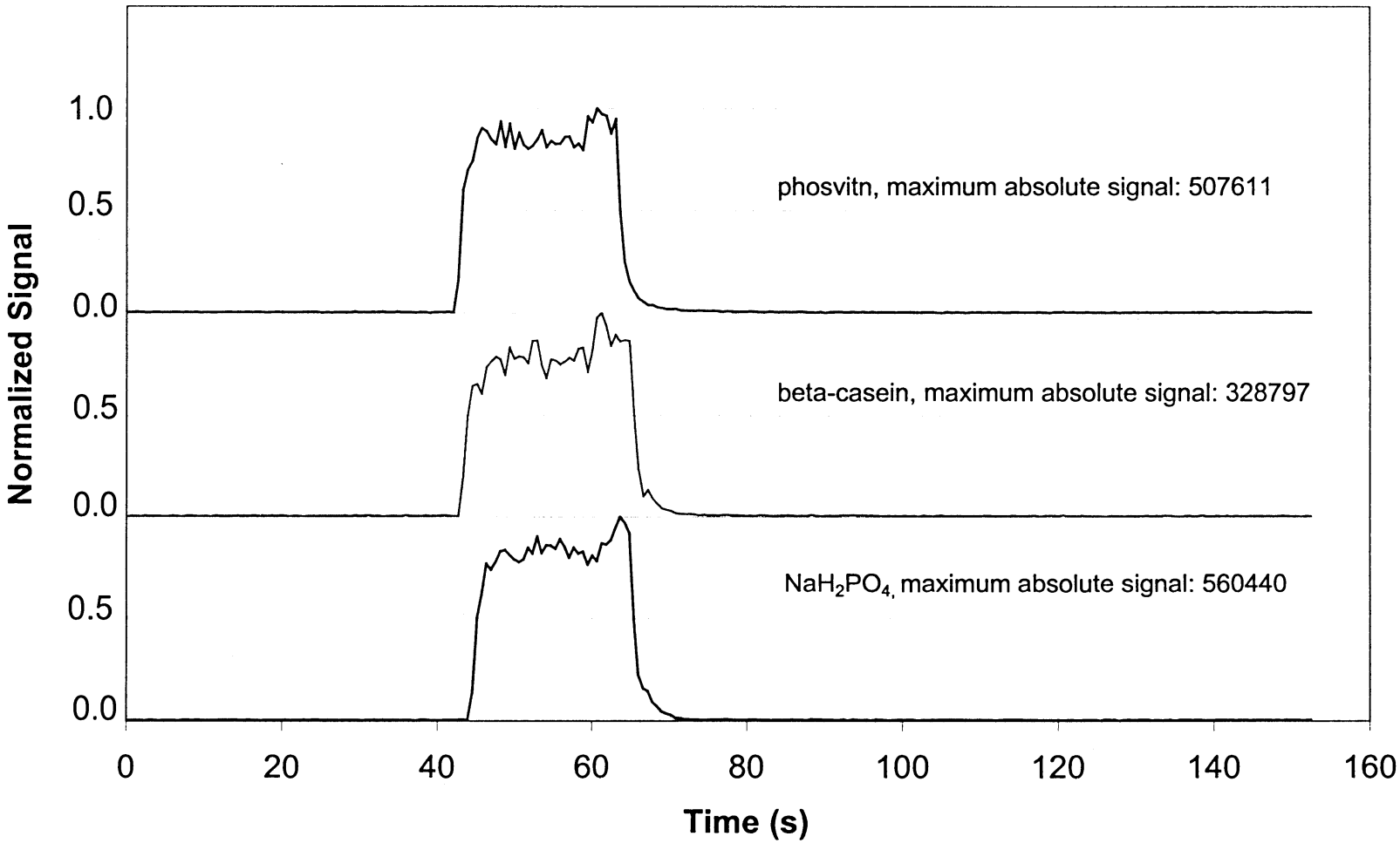

Fig 4A Rinse-Out curve of three samples, PFA nebulizer, natural uptake

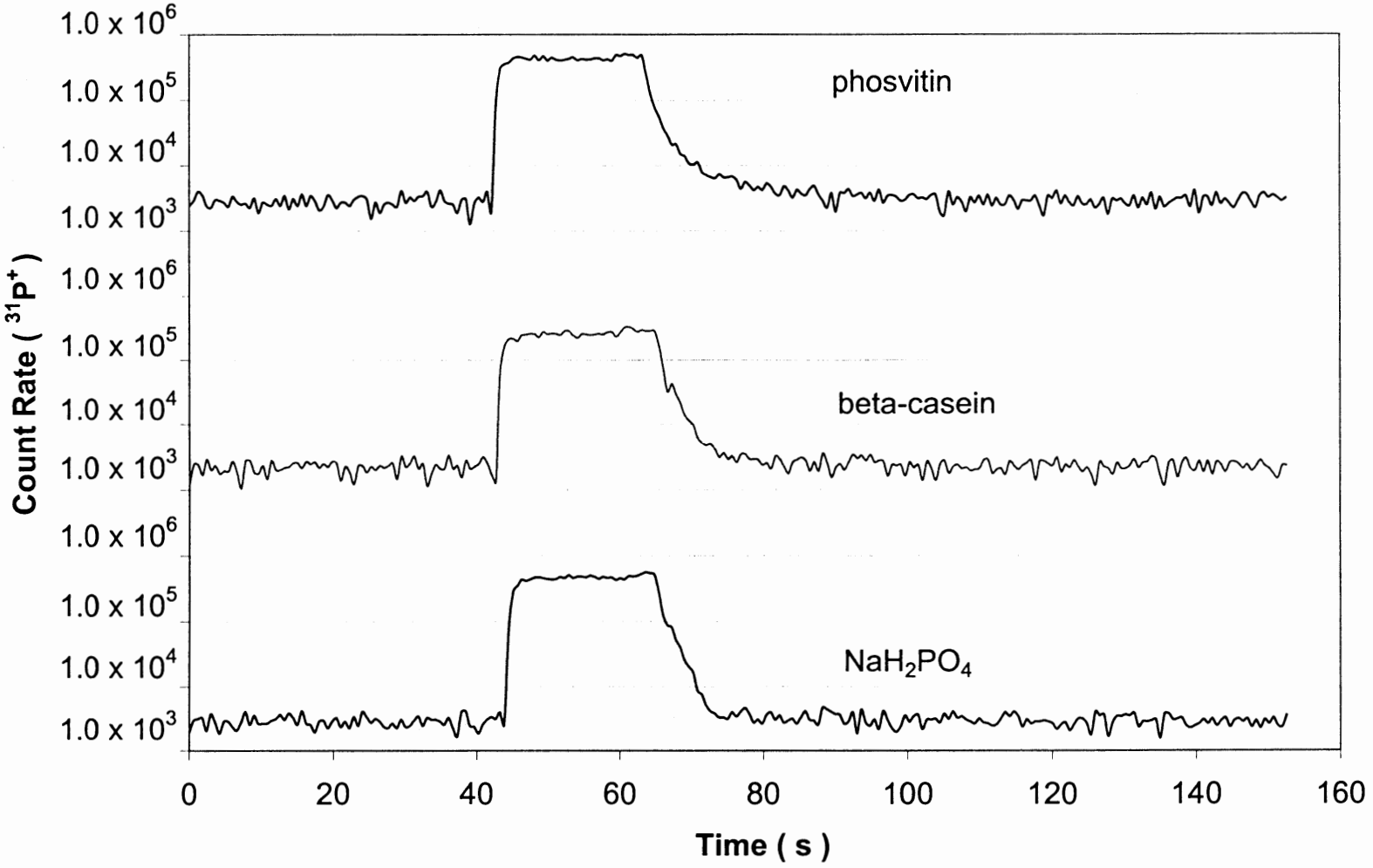

Fig 4B Log View, Rinse-Out curve of three samples, PFA nebulizer, natural uptake

4. GENERAL CONCLUSION

ICP-MS is a wonderful technique for trace and ultra-trace elemental analysis. Thanks to the modern electronics and computerized automation, ICP-MS instrument is getting more efficient, stable, sensitive and accurate. The combination of ICP-MS with other techniques, such as liquid chromatography makes ICP-MS more powerful and charming.

SEC column supplies an amicable condition for bio-molecules. Separations happening in SEC column with proper buffers are not supposed to hurt the activeness or attributes of bio-molecules. In this work, uranium and holmium at low ppb level was spiked to DNA mixture at ppm level. Since both the reaction and separation occurred in buffer, this work imitated what could be happening between DNA and the two metals under natural conditions. The SEC column separated fragments of DNA mixtures and supplied information about the sizes of fragments; the ICP-MS machine confidently measured the very low amount of metals possibly bound to DNA fragments; the serial measurements helped us make the dynamic investigations on the uranium/holmium-DNA interactions. The understanding of how uranium and post-uranium elements interact with DNA has important meaning to human health, environmental protection and industry/military usage. That is why we did the research and what we wanted to get from it. Hopefully, we can even use SEC-ICP-MS for other dynamic explorations regarding the metal-biomolecules interactions.

Quantifying phosphorous in proteins is tremendously important to the research in phosphoprotein. ICP-MS turns out to be a reliable and accurate technique for this task. According to the aerosol flow rate experiments, protein can be dissociated, atomized and ionized similarly as inorganic phosphate was. This means ICP as ionization source is strong enough to equally and quantitatively convert protein into the detectable forms of ICP-MS.

The test with phosvitin gave a good proof to our methodology. The test with β-casein was off by 50%. We suspect some phosphorous of β-casein was lost during purification so that our sample β-casein never had as much phosphorous as expected. The detection limit of phosphorous with Element ICP-MS can be as low as 8 pg if the spectrum method is in use and it can be as low as 20 pg if the flow injection method is in use.

ACKNOWLEDGEMENTS

First and foremost, I would like to express my deep sincere appreciation to my major professor, Dr. R. S. Houk, for his support, tolerance and guidance both in graduate courses and my research. Without him, none of those work can be done.

Sincere thanks is also extended to Dr. Edward Yeung and Dr. Cheuk-Yiu Ng, who serve as my committee members. Their critical reading of this manuscript and suggestions are greatly appreciated.

I would like to thank Dr. Joseph Burnett, supervisor of CHEM 211. I enjoy being his teaching assistant and thank him very much for his opening the CHEM 211 facility to my experiments.

I would like to thank all the members in Dr. Houk's group. In particular, thank David Aeschliman for teaching me how to use Element, thank Towhid Hasan for the helpful discussion on research, and thank Fumin Li and Kent Geoffrey for friendship.

I owe deep gratitude to my wife Jing Zheng and my parents for their unconditional love and emotional support.

Finally, my sincere thanks go to Iowa State University and Ames Laboratory for their financial support.